PHYSICAL REVIEW D VOLUME 44, NUMBER 6 15 SEPTEMBER 1991

Discretized light-cone quantization: Formalism for quantum electrodynamics

Andrew C. Tang and Stanley J. Brodsky
Stanford Linear Accelerator Center, Stanford University, Stanford, California 94309

Hans-Christian Pauli
Max-Planck-Institut für Kernphysik, D-6900 Heidelberg 1, Germany
(Received 8 March 1991)

A general nonperturbative method for solving quantum field theories in three space and one time dimensions, discretized light-cone quantization, is outlined and applied to quantum electrodynamics. This numerical method is frame independent and can be formulated such that ultraviolet regularization is independent of the momentum-space discretization. In this paper we discuss the construction of the light-cone Fock basis, ultraviolet regularization, infrared regularization, and the renormalization techniques required for solving QED as a light-cone Hamiltonian theory.

I. INTRODUCTION

Perhaps the most outstanding problem in quantum field theory is to compute the bound-state spectrum and the relativistic wave functions of hadrons at strong coupling. In quantum chromodynamics one needs a practical computational method which not only determines the hadronic and exotic spectra, but also can provide nonperturbative hadronic matrix elements of the operator-product expansion, weak decay amplitudes, structure functions, and distribution amplitudes. In general, the computation of hadronic scattering amplitudes requires knowledge of the bound-state wave functions at arbitrary four-momentum. Lattice gauge theory has provided important tools for analyzing the lowest hadronic states of quantum chromodynamics (QCD), but detailed wave-function information has been very difficult to obtain.

Even in the case of Abelian quantum electrodynamics, very little is known about the nature of the bound-state solutions in the large-α, strong-coupling, domain. The Bethe-Salpeter formalism has been the central method for analyzing hydrogenic atoms in quantum electrodynamics (QED), providing a completely covariant procedure for obtaining bound-state solutions. However, calculations using this method are extremely complex and appear to be intractable much beyond the ladder approximation. It also appears impractical to extend this method to systems with more than a few constituent particles.

The most intuitive approach for solving relativistic bound-state problems would be to solve the Hamiltonian eigenvalue problem for field theories

$$H|\psi\rangle=\sqrt{\mathbf{P}^2+M^2}\,|\psi\rangle \tag{1.1}$$

for the particle's mass M and wave function $|\psi\rangle$. Here, one imagines that $|\psi\rangle$ is an expansion in multiparticle occupation-number Fock states and that the operators H and $\mathbf{P}$ are second-quantized Heisenberg picture operators. Unfortunately, this method, as described by Tamm and Dancoff [1], is severely complicated by its noncovariance and the necessity to first understand its complicated vacuum eigensolution over all space and time. The presence of the square-root operator also presents severe mathematical difficulties. Even if these problems could be solved, the eigensolution is only determined in its rest system; determining the boosted wave function is as complicated as diagonalizing H itself. Fortunately, "light-cone" quantization offers an elegant avenue of escape. The square-root operator does not appear in light-cone formalism, and as we will see explicitly in Sec. II, the structure of the vacuum does not play an important role in QED since there is no spontaneous creation of massive fermions in the light-cone quantized vacuum.

There are, in fact, many reasons to quantize relativistic field theories at light-cone time. Dirac [2], in 1949, showed that a maximum number of Poincaré generators become independent of the dynamics in the "front-form" formulation, including the required Lorentz boosts. In fact, unlike the traditional equal-time Hamiltonian formalism, quantization of the light cone can be formulated without reference to the choice of a specific Lorentz frame; the eigensolutions of the light-cone Hamiltonian thus describe bound states of arbitrary four-momentum, allowing the computation of scattering amplitudes and other dynamical quantities. However, the most remarkable feature of this formalism for $(3+1)$-dimensional QED (QED_{3+1}) is the simplicity of the light-cone vacuum. The vacuum state of the free Hamiltonian is the vacuum eigenstate of the total light-cone Hamiltonian. The Fock expansion constructed on this vacuum state provides a complete relativistic many-particle basis for diagonalizing the full theory.

In this paper we will quantize quantum electrodynamics on the light cone in a discretized form which allows practical numerical solutions for obtaining its spectrum and wave functions at arbitrary coupling strength α. Hopefully, these techniques will be applicable to non-Abelian gauge theories, including quantum chromodynamics in physical space time. In this paper, we discuss the ultraviolet and infrared regularization of the theory which renders it finite. In addition to momentum-space regularization, we also discuss a co-

variant approximately gauge-invariant particle number truncation of the Fock basis which is useful both for computational purposes and physical approximations. In this method, "discretized light-cone quantization" (DLCQ) [3], ultraviolet and infrared regularizations are kept independent of the discretization procedure and are identical to that of the continuum theory. One thus obtains a finite discrete representation of the gauge theory which is faithful to the continuum theory and is completely independent of the choice of Lorentz frame. Recently, Wilson *et al.* have developed a complimentary method, the light-front Tamm-Dancoff approach [4,5] which uses a fixed-number Fock basis to truncate the theory. Wilson has also emphasized the potential advantages of using a Gaussian basis similar to that used in many-electron molecular systems for relativistic many-body light-cone problems rather than the plane-wave basis used here [5]. A discussion of the numerical methods which can be used to solve the DLCQ system and initial results for the positronium spectrum in QED_{3+1} at moderate values of α will be given in Ref. [6].

The possibility of quantizing on the light cone was first discovered by Dirac [2]. The striking advantages of this formalism for gauge theory have been realized by a number of authors, including Klauder, Leutwyler, and Streit [7], Kogut and Soper [8], Rohrlich [9], Leutwyler [10], Casher [11], Chang, Root, and Yan [12], Lepage and Brodsky [13], Brodsky and Ju [14], Lepage, Brodsky, Huang, and Mackenzie [15], and McCartor [16]. Leutwyler recognized the utility of defining quark wave functions on the light cone to give an unambiguous meaning to concepts used in the parton model. Casher gave the first construction of the light-cone Hamiltonian for non-Abelian gauge theory and gave an overview of important considerations in light-cone quantization. Chang, Root, and Yan demonstrated the equivalence of light-cone quantization with standard covariant Feynman analysis.

There has also been important work on light-cone quantization by Franke [17–19], Karmanov [20,21], and Pervushin [22]. The notation used in this paper is given in Table I. A comparison of light-cone quantization with equal-time quantization is shown in Table II.

The question of whether boundary conditions can be consistently set in light-cone quantization has been discussed by McCartor [23] and Lenz [24]. They have also shown that, for massive theories, the energy and momentum derived using light-cone quantization are not only conserved, but also are equivalent to the energy and momentum one would normally write down in an equal-time theory.

TABLE I. Definitions in light-cone quantization.

Variables	τ=light-cone time$=x^+=x^0+x^3$ x^-=light-cone position$=x^0-x^3$ $\mathbf{x}_\perp=(x^1,x^2)$
Covariant notation	$A^\mu=(A^+,A^-,\mathbf{A}_\perp)$
Metric	$(g^{\mu\nu})=\begin{bmatrix}0&2&0&0\\2&0&0&0\\0&0&-1&0\\0&0&0&-1\end{bmatrix}$
Dot product	$x\cdot y=x^\mu g_{\mu\nu}y^\nu=\frac{1}{2}(x^+y^-+x^-y^+)-\mathbf{x}_\perp\cdot\mathbf{y}_\perp$
Mass-shell condition	$P^+P^-=\mathbf{P}_\perp^2+M^2$
Derivative	$\partial_+=\frac{\partial}{\partial x^+}$, $\partial_-=\frac{\partial}{\partial x^-}$, $\partial_i=\frac{\partial}{\partial x_i}$ $\partial^+=2\partial_-$, $\partial^-=2\partial_+$, $\partial^i=-\partial_i$
Underscore notation	$\underline{x}=(x^-,\mathbf{x}_\perp)$, $\underline{k}=(k^-,\mathbf{k}_\perp)$ $\underline{k}\cdot\underline{x}=\frac{1}{2}k^+x^--\mathbf{k}_\perp\cdot\mathbf{x}_\perp$

The approach that we use in this paper is closely related to the light-cone Fock methods used in Ref. [13] in the analysis of exclusive processes in QCD. The renormalization of light-cone wave functions and the calculation of physical observables in the light-cone framework is also discussed in that paper. The analysis of light-cone perturbation theory rules for QED in the light-cone gauge used here is similar to that given in Ref. [25]. A number of other applications of QCD in light-cone quantization are reviewed in Ref. [26].

A mathematically similar but conceptually different approach to light-cone quantization is the "infinite-momentum-frame" formalism. This method involves observing the system in a frame moving past the laboratory close to the speed of light. The first developments were given by Weinberg [27]. Although light-cone quantization is similar to infinite-momentum-frame quantization, it differs since no reference frame is chosen for calculations, and it is thus manifestly Lorentz covariant. The only aspect that "moves at the speed of light" is the quantization surface. Other works in infinite-momentum-frame physics include Drell, Levy, and Yan [28], Susskind and Frye [29], Bjorken, Kogut, and Soper [30], and Brodsky, Roskies, and Suaya [31]. This last reference presents the infinite-momentum-frame pertur-

TABLE II. A comparison of light-cone and equal-time quantization.

	Instant form	Front form
Hamiltonian	$H=\sqrt{\mathbf{P}^2+m^2}+V$	$P^-=\frac{P_\perp^2+m^2}{P^+}+V$
Conserved quantities	$E,\mathbf{P}$	$P^-,P^+,\mathbf{P}_\perp$
Momenta	$-\infty<P_z<\infty$	$P^+>0$
Bound-state equation	$H\psi=E\psi$	$(P^+P^--P_\perp^2)\psi=M^2\psi$
Vacuum (QED)	Complicated	"Trivial"

bation theory rules for QED in the Feynman gauge, calculates one-loop radiative corrections, and demonstrates renormalizability.

In order to capitalize on the features of light-cone quantization, Pauli and Brodsky [3] developed the method of discretized light-cone quantization and applied it to solving for the mass spectrum and wave functions of Yukawa theory $\bar{\psi}\psi\phi$, in one space and one time dimensions. This success leads to further applications including QED_{1+1} and the Schwinger model by Eller, Pauli, and Brodsky [32] ϕ^4 theory in 1+1 dimensions by Harindranath and Vary [33], and QCD_{1+1} for $N_C=2$, 3, and 4 by Hornbostel, Brodsky, and Pauli [34]. Burkardt [35] has used related light-cone integral equation methods to obtain the hadron spectrum in QCD_{1+1} as well as to study European Muon Collaboration (EMC)-like effects in nuclear structure functions in that theory. More recently, Burkardt and Busch [36] have studied flavor-breaking effects in the Gottfried sum rule in QCD_{1+1}. In each of these applications, the mass spectrum and wave functions were successfully obtained, and all results agree with previous analytical and numerical work, where they were available. Recently, Hiller [37] has used DLCQ and the Lanczos algorithm for matrix diagonalization method to compute the annihilation cross section, structure functions, and form factors in a (1+1)-dimensional Yukawa theory.

The initial successes of DLCQ provide the hope that one can use this method for solving 3+1 theories. The application to higher dimensions is much more involved due to the need to introduce ultraviolet and infrared regulators, and invoke a renormalization scheme consistent with gauge invariance and Lorentz invariance. This is in addition to the work involved implementing two extra dimensions with their added degrees of freedom. In this paper, we will present the application of DLCQ to (3+1)-dimensional QED.

The basic background for light-cone quantization and DLCQ is shown in Refs. [3], [32], and Secs. 2 and 3 of Ref. [38]. The light-cone Hamiltonian for (3+1)-dimensional QED is given in Sec. II, ultraviolet regularization in Sec. III, and infrared regularization in Sec. IV. Section III also introduces a method for maintaining gauge invariance of the ultraviolet regulator, at least for tree-level fermion-fermion scattering. It is important to maintain gauge invariance and the Lorentz boost symmetries when truncating the Fock space. A method for preserving these symmetries while truncating the Fock-space basis is presented in Sec. V. Renormalization in this truncated space is discussed in Sec. IV. The question of self-induced inertias and the equivalence of Feynman rules and light-cone perturbation theory results for one-loop mass counterterms is also presented in Sec. VI. A number of mathematical details are given in the various appendices.

II. LIGHT-CONE QUANTIZATION OF QED

The derivation of the light-cone Hamiltonian H_{LC} from the (3+1)-dimensional QED Lagrangian,

$$\mathcal{L}=\frac{i}{2}[\bar{\psi}\gamma^{\mu}\partial_{\mu}-(\partial_{\mu}\bar{\psi})\gamma^{\mu}]\psi-m_e\bar{\psi}\psi -\tfrac{1}{4}F_{\mu\nu}F^{\mu\nu}-g\bar{\psi}\gamma^{\mu}\psi A_{\mu}\ , \tag{2.1}$$

can be carried out in the light-cone gauge $A^{+}=A^{0}+A^{3}=0$ using the standard methods of canonical quantization with (anti)periodic boundary conditions. The procedure and notation closely follow the quantization of QCD in one space and one time dimension. See Ref. [34]. Details of this derivation for $\mathrm{QED}_{(3+1)}$ are given in Sec. IV of Ref. [38]. In a general frame, we write

$$P^{-}=\frac{H_{\mathrm{LC}}+P_{\perp}^2}{P^{+}}$$

so that the eigenvalues of H_{LC} give the invariant-mass spectrum M^2. The result after using the classical equations of motion to eliminate the dependent fields ψ_{-} and A^{-}, imposing canonical commutation relations on the independent fields ψ_{+} and $\mathbf{A}_{\perp}$, and finally discretizing these two fields by expanding in plane waves and imposing boundary conditions is

$$H_{\mathrm{LC}}=H_0+H_1+H_2\ ,$$
$$H_1=V_{\mathrm{flip}}+V_{\mathrm{nonflip}},\quad H_2=V_{\mathrm{instphot}}+V_{\mathrm{instferm}}\ , \tag{2.2}$$

$$H_0=\sum_{\lambda,p}\frac{K}{p}\left[\left[\frac{p_{\perp}\pi}{L_{\perp}}\right]^2+\lambda^2\right]a^{\dagger}_{\lambda,\underline{p}}a_{\lambda,\underline{p}}+\sum_{s,\underline{n}}\frac{K}{n}\left[\left[\frac{n_{\perp}\pi}{L_{\perp}}\right]^2+m_e^2\right](b^{\dagger}_{s,\underline{n}}b_{s,\underline{n}}+d^{\dagger}_{s,\underline{n}}d_{s,\underline{n}})\ , \tag{2.3}$$

$$V_{\mathrm{flip}}=g\frac{Km_e}{2\sqrt{\pi}L_{\perp}}\sum_{s}\sum_{\underline{p},\underline{m},\underline{n}}\frac{1}{\sqrt{p}}\left[+a_{2s,\underline{p}}b^{\dagger}_{s,\underline{m}}b_{-s,\underline{n}}\delta^{(3)}_{\underline{n}+\underline{p},\underline{m}}\left[\frac{1}{n}-\frac{1}{m}\right]+\mathrm{H.c.}\right.$$
$$\left.-a_{2s,\underline{p}}d^{\dagger}_{s,\underline{m}}d_{-s,\underline{n}}\delta^{(3)}_{\underline{n}+\underline{p},\underline{m}}\left[\frac{1}{n}-\frac{1}{m}\right]+\mathrm{H.c.}+a^{\dagger}_{2s,\underline{p}}b_{s,\underline{m}}d_{s,\underline{n}}\delta^{(3)}_{\underline{n}+\underline{m},\underline{p}}\left[\frac{1}{n}+\frac{1}{m}\right]+\mathrm{H.c.}\right]\ , \tag{2.4}$$

$$V_{\text{nonflip}}=g\left[\frac{\pi}{2}\right]^{1/2}\frac{K}{L_\perp^2}\sum_s\sum_{\underline{p},\underline{m},\underline{n}}\frac{1}{\sqrt{\underline{p}}}\left[a_{2s,\underline{p}}b^\dagger_{s,\underline{m}}b_{s,\underline{n}}\delta^{(3)}_{\underline{n}+\underline{p},\underline{m}}\epsilon^\perp_{2s}\cdot\left[\frac{\mathbf{p}_\perp}{p}-\frac{\mathbf{n}_\perp}{n}\right]+\text{H.c.}\right.$$
$$+a_{-2s,\underline{p}}b^\dagger_{s,\underline{m}}b_{s,\underline{n}}\delta^{(3)}_{\underline{n}+\underline{p},\underline{m}}\epsilon^\perp_{-2s}\cdot\left[\frac{\mathbf{p}_\perp}{p}-\frac{\mathbf{m}_\perp}{m}\right]+\text{H.c.}$$
$$-a_{2s,\underline{p}}d^\dagger_{s,\underline{m}}d_{s,\underline{n}}\delta^{(3)}_{\underline{n}+\underline{p},\underline{m}}\epsilon^\perp_{2s}\cdot\left[\frac{\mathbf{p}_\perp}{p}-\frac{\mathbf{n}_\perp}{n}\right]+\text{H.c.}$$
$$-a_{-2s,\underline{p}}d^\dagger_{s,\underline{m}}d_{s,\underline{n}}\delta^{(3)}_{\underline{n}+\underline{p},\underline{m}}\epsilon^\perp_{-2s}\cdot\left[\frac{\mathbf{p}_\perp}{p}-\frac{\mathbf{m}_\perp}{m}\right]+\text{H.c.}$$
$$-a^\dagger_{2s,\underline{p}}b_{s,\underline{m}}d_{-s,\underline{n}}\delta^{(3)}_{\underline{n}+\underline{m},\underline{p}}\epsilon^{*\perp}_{2s}\cdot\left[\frac{\mathbf{p}_\perp}{p}-\frac{\mathbf{n}_\perp}{n}\right]+\text{H.c.}$$
$$\left.-a^\dagger_{-2s,\underline{p}}b_{s,\underline{m}}d_{-s,\underline{n}}\delta^{(3)}_{\underline{n}+\underline{m},\underline{p}}\epsilon^{*\perp}_{-2s}\cdot\left[\frac{\mathbf{p}_\perp}{p}-\frac{\mathbf{m}_\perp}{m}\right]+\text{H.c.}\right], \tag{2.5}$$

$$V_{\text{instphot}}=g^2\frac{K}{2\pi L_\perp^2}\sum_{s,t}\sum_{\underline{k},\underline{l},\underline{m},\underline{n}}(-b^\dagger_{s,\underline{k}}b^\dagger_{t,\underline{l}}b_{s,\underline{m}}b_{t,\underline{n}}\delta^{(3)}_{\underline{l}+\underline{k},\underline{m}+\underline{n}}\tfrac{1}{2}[k-m|-l+n]$$
$$-d^\dagger_{s,\underline{k}}d^\dagger_{t,\underline{l}}d_{s,\underline{m}}d_{t,\underline{n}}\delta^{(3)}_{\underline{k}+\underline{l},\underline{m}+\underline{n}}\tfrac{1}{2}[k-m|-l+n]$$
$$-b^\dagger_{s,\underline{k}}d^\dagger_{-s,\underline{l}}b_{t,\underline{m}}d_{-t,\underline{n}}\delta^{(3)}_{\underline{k}+\underline{l},\underline{m}+\underline{n}}[k+l|m+n]$$
$$+b^\dagger_{s,\underline{k}}d^\dagger_{-t,\underline{l}}b_{s,\underline{m}}d_{-t,\underline{n}}\delta^{(3)}_{\underline{k}+\underline{l},\underline{m}+\underline{n}}[k-m|-l+n]$$
$$+d^\dagger_{s,\underline{k}}d_{t,\underline{l}}d_{s,\underline{m}}b_{-t,\underline{n}}\delta^{(3)}_{\underline{k},\underline{l}+\underline{m}+\underline{n}}[k-m|l+n]+\text{H.c.}$$
$$+b^\dagger_{s,\underline{k}}b_{t,\underline{l}}b_{s,\underline{m}}d_{-t,\underline{n}}\delta^{(3)}_{\underline{k},\underline{l}+\underline{m}+\underline{n}}[k-m|l+n]+\text{H.c.}), \tag{2.6}$$

$$V_{\text{instferm}}=g^2\frac{K}{4\pi L_\perp^2}\sum_s\sum_{\underline{p},\underline{q},\underline{m},\underline{n}}\frac{1}{\sqrt{\underline{p}\underline{q}}}(+a^\dagger_{-2s,\underline{p}}a_{-2s,\underline{q}}b^\dagger_{s,\underline{m}}b_{s,\underline{n}}\delta^{(3)}_{\underline{p}+\underline{m},\underline{q}+\underline{n}}\{p+m|q+n\}$$
$$-a^\dagger_{2s,\underline{p}}a_{2s,\underline{q}}b^\dagger_{s,\underline{m}}b_{s,\underline{n}}\delta^{(3)}_{\underline{p}+\underline{m},\underline{q}+\underline{n}}\{p-n|q-m\}$$
$$+a^\dagger_{-2s,\underline{p}}a_{-2s,\underline{q}}d^\dagger_{s,\underline{m}}d_{s,\underline{n}}\delta^{(3)}_{\underline{p}+\underline{m},\underline{q}+\underline{n}}\{p+m|q+n\}$$
$$-a^\dagger_{2s,\underline{p}}a_{2s,\underline{q}}d^\dagger_{s,\underline{m}}d_{s,\underline{n}}\delta^{(3)}_{\underline{p}+\underline{m},\underline{q}+\underline{n}}\{p-n|q-m\}$$
$$-a^\dagger_{2s,\underline{p}}a^\dagger_{-2s,\underline{q}}b_{s,\underline{m}}d_{-s,\underline{n}}\delta^{(3)}_{\underline{p}+\underline{q},\underline{m}+\underline{n}}\{p-m|-q+n\}+\text{H.c.}$$
$$-a^\dagger_{2s,\underline{p}}a_{2s,\underline{q}}b_{-s,\underline{m}}d_{s,\underline{n}}\delta^{(3)}_{\underline{p},\underline{q}+\underline{m}+\underline{n}}\{p-n|q+m\}+\text{H.c.}$$
$$+a^\dagger_{2s,\underline{p}}a_{2s,\underline{q}}b_{s,\underline{m}}d_{-s,\underline{n}}\delta^{(3)}_{\underline{p},\underline{q}+\underline{m}+\underline{n}}\{p-m|q+n\}+\text{H.c.}$$
$$-a_{-2s,\underline{p}}a_{2s,\underline{q}}b^\dagger_{s,\underline{m}}b_{s,\underline{n}}\delta^{(3)}_{\underline{m},\underline{p}+\underline{q}+\underline{n}}\{p+n|-q+m\}+\text{H.c.}$$
$$-a_{-2s,\underline{p}}a_{2s,\underline{q}}d^\dagger_{s,\underline{m}}d_{s,\underline{n}}\delta^{(3)}_{\underline{m},\underline{p}+\underline{q}+\underline{n}}\{p+n|-q+m\}+\text{H.c.}). \tag{2.7}$$

V_{flip} is the spin-flip amplitude for a (anti) fermion to (absorb) emit a photon and V_{nonflip} is the no-spin-flip amplitude for this process. The familiar three-point Dirac QED vertex is just the sum of these two amplitudes. Two other types of vertices appear in light-cone quantization: a four-point instantaneous photon exchange, V_{instphot}, and a four-point instantaneous fermion exchange, V_{instferm}. These are just the graphs needed to reproduce the usual covariant Feynman S-matrix results for scattering amplitudes. An example of this for Møller scattering ($e^-e^-\to e^-e^-$) is shown in Appendix A. One can think of the instantaneous photon exchange graph in light-cone gauge as being analogous to the Coulomb exchange graph in Coulomb gauge. All the interactions conserve k^+ and $\mathbf{k}_\perp$, as they must, and are shown schematically in Fig. 1.

In the above expression for H_{LC}, g is the coupling constant, $2L_\perp$ is the size of the transverse box, λ is an artificial photon mass which is ultimately set equal to zero and, as will be explained shortly, K is related to the value of P^+. The expression has also been normal-ordered to remove vacuum values and self-induced inertias (more on these in Sec. VI). The integers $p,q,m,n,\ldots$ are allowed to take on the values

$$p^i,q^i,k^i,l^i,m^i,n^i=0,\pm1,\pm2,\ldots,\quad i=1,2\ ,$$
$$p,q=2,4,6,\ldots,$$
$$k,l,m,n=\begin{cases}2,4,6,\ldots & \text{[periodic boundary condition (BC)]},\\ 1,3,5,\ldots & \text{(antiperiodic BC)}\ .\end{cases}\tag{2.8}$$

$[n|m]$ and $\{n|m\}$ were first defined in Ref. [32]. A modified version using a method suggested by Hamer [39] based on the form of the Lagrangian, Eq. (2.1), leads to

$$[n|m]=\begin{cases}\dfrac{1}{n^2}\delta_{n,m}, & n,m\neq0,\\ \kappa, & n \text{ and } m=0,\\ 0, & \text{otherwise}\ ,\end{cases}$$
$$\{n|m\}=\begin{cases}\dfrac{1}{n}\delta_{n,m}, & n,m\neq0,\\ 0, & n \text{ or } m=0\ .\end{cases}\tag{2.9}$$

Details can be found in Sec. IV and Appendix B of Ref. [38]. Since the gauge-invariant cutoff introduced in Sec. III eliminates all occurrences of $[0|0]$, the value of the unknown constant κ can be set equal to zero.

The free fermion and photon spinors are [40]

$$\chi(\uparrow)=\frac{1}{\sqrt{2}}\begin{bmatrix}1\\0\\1\\0\end{bmatrix},\quad \chi(\downarrow)=\frac{1}{\sqrt{2}}\begin{bmatrix}0\\1\\0\\-1\end{bmatrix},$$
$$\epsilon_\perp(\uparrow)=\frac{-1}{\sqrt{2}}(1,i),\quad \epsilon_\perp(\downarrow)=\frac{1}{\sqrt{2}}(1,-i)\ ,\tag{2.10}$$

and the fermion and photon fields have discrete momenta in the x^- and x^i, $i=1,2$, directions due to the boundary conditions

photons:

$$k^i=\frac{p^i\pi}{L_\perp},\quad p^i=0,\pm1,\pm2,\ldots,$$
$$k^+=\frac{p\pi}{L},\quad p=2,4,6,\ldots,\tag{2.11}$$

fermions:

$$k^i=\frac{n^i\pi}{L_\perp},\quad n^i=0,\pm1,\pm2,\ldots,$$
$$k^+=\frac{n\pi}{L},\quad n=\begin{cases}2,4,6,\ldots & \text{(periodic BC)},\\ 1,3,5,\ldots & \text{(antiperiodic BC)}\ .\end{cases}$$

We have chosen periodic boundary conditions for the photon field $\mathbf{A}_\perp$ in the x^- and $\mathbf{x}_\perp$ directions, and periodic boundary conditions for the fermion field ψ_+ in the $\mathbf{x}_\perp$ directions. ψ_+ may have periodic or antiperiodic boundary conditions in the x^- direction. In the rest of this paper, antiperiodic conditions will be used. Note that only positive k^+ are allowed. This is because the mass-shell condition

$$k^-=\frac{k_\perp^2+m^2}{k^+}\tag{2.12}$$

only allows for k^+ and k^- both positive or both negative. As one does in equal-time considerations, the modes with negative energy (in our case, negative k^-) are redefined to be antiparticles (the photon is its own antiparticle). The result is that, in light-cone quantization, one only has states with both positive k^+ *and* positive k^-.

The above expression for $H_{\rm LC}$ is still incomplete due to the need to include fermion mass renormalization counterterms (see Sec. VI). We also note that $H_{\rm LC}$ is independent of the longitudinal box size L. This last result arises because P^+ is proportional to $1/L$ and P^- is proportional to L.

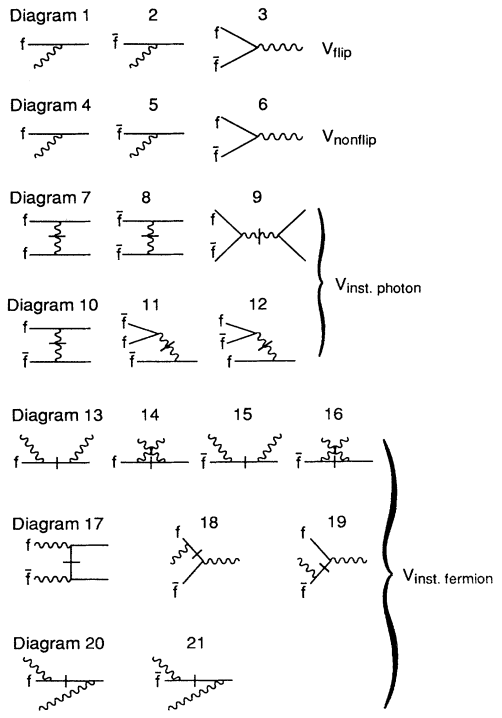

FIG. 1. Light-cone diagrams for QED interactions.

Other conserved quantities in the theory include the charge [41], light-cone momentum, and transverse momentum. The expressions for these in light-cone quantum mechanics after normal ordering to remove vacuum values are

$$Q=g\sum_{s,\underline{n}}(b^{\dagger}_{s,\underline{n}}b_{s,\underline{n}}-d^{\dagger}_{s,\underline{n}}d_{s,\underline{n}})\ ,$$
$$P^{+}=\sum_{\lambda,\underline{p}}k^{+}a^{\dagger}_{\lambda,\underline{p}}a_{\lambda,\underline{p}}+\sum_{s,\underline{n}}k^{+}(b^{\dagger}_{s,\underline{n}}b_{s,\underline{n}}+d^{\dagger}_{s,\underline{n}}d_{s,\underline{n}})\ , \quad (2.13)$$
$$P^{i}=\sum_{\lambda,\underline{p}}k^{i}a^{\dagger}_{\lambda,\underline{p}}a_{\lambda,\underline{p}}+\sum_{s,\underline{n}}k^{i}(b^{\dagger}_{s,\underline{n}}b_{s,\underline{n}}+d^{\dagger}_{s,\underline{n}}d_{s,\underline{n}})\ .$$

The last two equations are just statements of k^{+} and $\mathbf{k}_{\perp}$ momentum conservation: P^{+} is just the sum of the individual k^{+}'s and $\mathbf{P}_{\perp}$ is just the sum of the individual $\mathbf{k}_{\perp}$'s. These expressions are especially simple, and since they are already diagonal, the wave function $|\psi\rangle$ can immediately be chosen as an eigenstate of them. For convenience we can choose $P^{+}=2m_e$ and $\mathbf{P}_{\perp}=\mathbf{0}_{\perp}$ corresponding to the positronium center of mass and obtain

$$\left[\sum_{\lambda,\underline{p}}pa^{\dagger}_{\lambda,\underline{p}}a_{\lambda,\underline{p}}+\sum_{s,\underline{n}}n(b^{\dagger}_{s,\underline{n}}b_{s,\underline{n}}+d^{\dagger}_{s,\underline{n}}d_{s,\underline{n}})\right]|\psi\rangle=\frac{2m_eL}{\pi}|\psi\rangle=K|\psi\rangle\ ,$$
$$\left[\sum_{\lambda,\underline{p}}p^{i}a^{\dagger}_{\lambda,\underline{p}}a_{\lambda,\underline{p}}+\sum_{s,\underline{n}}n^{i}(b^{\dagger}_{s,\underline{n}}b_{s,\underline{n}}+d^{\dagger}_{s,\underline{n}}d_{s,\underline{n}})\right]|\psi\rangle=0|\psi\rangle\ , \quad (2.14)$$
$$p=2,4,6,\ldots,\quad n=1,3,5,\ldots\ \text{(antiperiodic BC)}\ ,$$
$$p^{i},n^{i}=0,\pm1,\pm2,\ldots\ .$$

From now on, only those expansion states satisfying these equations need be considered. In the first expression, the integer K is defined to be the eigenvalue P^{+} times L/π:

$$P^{+}=\frac{K\pi}{L}\ . \quad (2.15)$$

In Refs. [3] and [32], K is called the "harmonic resolution."

Finally observe that, because of k^{+} momentum conservation and the positivity of k^{+}, there are no interactions involving spontaneous creation or annihilation of a fermion pair and a photon from the vacuum. Because of this fact, the Fock-state vacuum (the state with no particles) is an eigenstate of the light-cone Hamiltonian with mass zero:

$$H_{\mathrm{LC}}|0\rangle=0|0\rangle\ . \quad (2.16)$$

This immensely simplifies solving for bound states because it removes the need to constantly recalculate the vacuum.

We now focus on the positronium bound-state problem. As in normal quantization we can apply the creation operators on the vacuum to create a complete light-cone Fock basis. The eigensolutions for the bound states will have the form

$$|\psi\rangle=\sum_{n}\psi_n(x,\mathbf{k}_{\perp})|n\rangle$$
$$=\psi_{e^{+}e^{-}}|e^{+}e^{-}\rangle+\psi_{e^{+}e^{-}\gamma}|e^{+}e^{-}\gamma\rangle+\cdots\ , \quad (2.17)$$

so that $\langle e^{+}e^{-}\gamma|\psi\rangle=\psi_{e^{+}e^{-}\gamma}(x,k_{\perp},\lambda)$. The labeling of the parton momenta for the positronium $e^{+}e^{-}\gamma$ Fock state is shown explicitly in Fig. 2. The sum is over all Fock states $|n\rangle$ with constituent momenta x_i and $\mathbf{k}_{\perp}$. In general, all Fock states are needed to describe the bound system; we will discuss the errors introduced by a truncation later. The Fock states are eigenstates of P^{+}, $\mathbf{P}_{\perp}$, and H_0. The $\mathbf{k}_{\perp i}$ and x_i are internal relative coordinates and are independent of the total momentum. The formalism is thus independent of the choice of reference frame. For calculational convenience, one can make the choice $\mathbf{P}_{\perp}=\mathbf{0}_{\perp}$, for which

$$P^{+}\left|n:k_i^{+},\mathbf{k}_{\perp i}\right\rangle=\frac{K\pi}{L}\left|n:k_i^{+},\mathbf{k}_{\perp i}\right\rangle\ ,$$
$$\mathbf{P}_{\perp}\left|n:k_i^{+},\mathbf{k}_{\perp i}\right\rangle=\mathbf{0}_{\perp}\left|n:k_i^{+},\mathbf{k}_{\perp i}\right\rangle\ , \quad (2.18)$$
$$H_0\left|n:k_i^{+},\mathbf{k}_{\perp i}\right\rangle=\sum_{i}\frac{k_{\perp i}^{2}+m_i^{2}}{x_i}\left|n:k_i^{+},\mathbf{k}_{\perp i}\right\rangle\ .$$

Because we are working with a discrete representation, the light-cone bound-state equation

$$H_{\mathrm{LC}}|m\rangle=M^{2}|m\rangle \quad (2.19)$$

can be converted into a matrix equation for the eigenvalues M^2 and eigenvectors ψ_n by projecting out the nth component:

$$\sum_{m}\langle n|H_{\mathrm{LC}}|m\rangle\psi_m(x_i,\mathbf{k}_{\perp,i},\lambda_i)=M^{2}\psi_n(x_u,\mathbf{k}_{\perp i},\lambda_i)\ . \quad (2.20)$$

For our case of positronium, the matrix equation is

$$\left[M^{2}-\sum_{i}\frac{k_{\perp i}^{2}+m_i^{2}}{x_i}\right]\begin{pmatrix}\psi_{e^{+}e^{-}}\\ \psi_{e^{+}e^{-}\gamma}\\ \vdots\end{pmatrix}=\begin{pmatrix}\cdots\\ \cdots\\ \ddots\end{pmatrix}\begin{pmatrix}\psi_{e^{+}e^{-}}\\ \psi_{e^{+}e^{-}\gamma}\\ \vdots\end{pmatrix}\ . \quad (2.21)$$

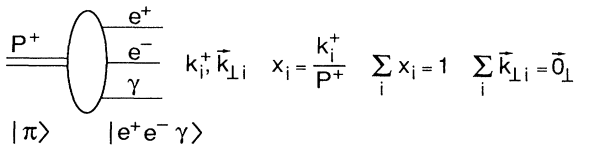

FIG. 2. Decomposition of positronium into Fock states.

Here, $H_{\rm LC}$ has been split into an interacting piece V and a noninteracting piece $H_0=\sum_i(k_{\perp i}^2+m_i^2/x_i)$. m_i is the mass of the ith constituent particle. For the case of positronium, it is either the fermion mass or the photon mass. Diagonalization of this equation can now be done on a computer (after implementing ultraviolet and infrared regulators) to reveal the complete spectrum of positronium states and multiparticle scattering states with the same quantum numbers, along with their corresponding wave-function expansion coefficients ψ_n. Solving the field theory has now been reduced to obtaining the solution to this fairly simple equation.

In summary, the discretized light-cone quantization procedure is straightforward. The light-cone Hamiltonian is derived from the Lagrangian by a procedure very similar to standard canonical quantization. The commuting operators, the light-cone momentum $P^+=K\pi/L$, transverse momentum $\mathbf{P}_\perp$, and light-cone Hamiltonian $H_{\rm LC}$ are constructed by expanding in Fock states and are simultaneously diagonalized. The expressions for P^+ and $\mathbf{P}_\perp$ are already diagonal if one expands in plane waves. The system is discretized by requiring periodic or antiperiodic boundary conditions in the light-cone spatial dimensions, and the system is quantized by imposing canonical commutation relations between the independent fields and their canonical momenta. The bound-state equation $H_{\rm LC}|\psi\rangle=M^2|\psi\rangle$ is diagonalized to obtain the invariant-mass spectrum and wave functions. Both of these quantities are independent of L. To recover the continuum theory, one lets K and $L_\perp$ approach infinity (this is equivalent to letting $L,L_\perp\to\infty$).

III. COVARIANT ULTRAVIOLET REGULATOR

Before continuing, a method of regulating the $\mathbf{k}_\perp$ Fock space and other ultraviolet divergences is necessary. The Fock space is naturally finite in k^+ because the total k^+ is just the sum of the individual, constituent k^+'s. Combining the fact that all the individual k^+'s are positive, nonzero integers with the fact that there are only a finite number of ways of summing a set of positive, nonzero integers to form a given positive number demonstrates finiteness of the k^+ space. As an example, a Fock state with one electron and two photons with $K=9$ can have the following quantum numbers (antiperiodic boundary conditions):

Fock state	1	2	3	4	5	6
Electron	1	1	1	3	3	5
Photon 1	2	4	6	2	4	2
Photon 2	6	4	2	4	2	2

In contrast with k^+, the Fock space is naturally infinite in $\mathbf{k}_\perp$ because $\mathbf{k}_\perp$ can take values that are positive or negative. An ultraviolet regulator must therefore be introduced.

We will discuss several possibilities for the frame-independent ultraviolet truncation of the light-cone Fock state. In the first method, which we refer to as the "global cutoff," we restrict the sum of the light-cone energies $(k_\perp^2+m^2)/x$ of the particles of each Fock state in a bound state to be less than a cutoff value Λ^2 (see Ref. [13]):

$$\sum_i \frac{k_{\perp i}^2+m_i^2}{x_i}\le\Lambda^2 . \tag{3.1}$$

The left-hand side of this equation is just the invariant-mass (for a single-particle state, the invariant mass is the rest mass) squared of the Fock state, $M^2=P^+P^--P_\perp^2$. It is also the value of the light-cone Hamiltonian at zero coupling. Thus, the global cutoff for the bound-state problem simply requires the invariant-mass squared of the individual Fock states to be less than Λ^2. For a scattering amplitude, the global cutoff limits the difference between the invariant mass of the initial and intermediate states. This regulator is invariant under the class of light-cone Lorentz transformations: rotations around the z direction, transverse boosts, and boosts in the z direction [42]. It should be emphasized that the variables $\mathbf{k}_{\perp i}$ and x_i are relative internal coordinates, independent of the total momentum P^+ and $\mathbf{P}_\perp$ of the bound state. The physical momentum of the particle in any given Lorentz frame is $\mathbf{p}_{\perp i}=\mathbf{k}_{\perp i}+x_i\mathbf{P}_\perp$ and $p^+=x_iP^+$.

Each Fock state is off the light-core energy shell by the amount

$$\sum_i k_i^- - P^- = \sum_i \left[\frac{(\mathbf{k}_{\perp i}+x_i\mathbf{P}_\perp)^2+m_i^2}{x_iP^+}\right]-\frac{P_\perp^2+M^2}{P^+}$$
$$=\frac{1}{P^+}\left[\sum_i\frac{k_{\perp i}^2+m_i^2}{x_i}-M^2\right]. \tag{3.2}$$

One sees immediately that the ultraviolet truncation given in Eq. (3.1) removes Fock states not by particle number but because they are far off shell. This is a reasonable procedure because far-off-shell states give only a small contribution to a physical wave function. It is known from general considerations [43] that the probability for high far-off-shell fluctuations of the renormalized wave function in a renormalizable theory are power-law suppressed, so that one expects convergence of all physical quantities as long as Λ is taken larger than all relevant mass scales of the problem. In fact, one sees from Eqs. (2.20) and (2.21) that a typical wave function in QED will have the form

$$\psi_n(x_i,\mathbf{k}_{\perp i},\lambda_i)=\frac{1}{M^2-\sum_i(k_{\perp i}^2+m_i^2)/x_i}(V\Psi) , \tag{3.3}$$

which tends to vanish as

$$\sum_i\frac{k_{\perp i}^2+m_i^2}{x_i}-M^2\to\infty . \tag{3.4}$$

In principle, one must make Λ infinite to recover the full theory. In practice, one can take moderate values of the cutoff and study the convergence of the spectrum and physical quantities as a function of Λ. In fact, since the binding energy is the relevant scale, it is more useful, in practice, to only restrict the kinetic part of the off-shell

energy. We thus define the "kinetic cutoff"

$$\sum_i \frac{k_{\perp i}^2+m_i^2}{x_i} - \min\left[\sum_i \frac{k_{\perp i}^2+m_i^2}{x_i}\right] \leq \Lambda^2 , \tag{3.5}$$

where the minimum is taken over all allowed kinematic configurations. By using the kinetic cutoff, states with high-momentum constituents are cut off, but fermion pair states which play an important role in Compton amplitudes are not preferentially excluded.

Cutting off the photon's momentum $\mathbf{k}_\perp$ is clearly not compatible with gauge invariance because the various graphs involved in photon exchange are cut off in a different way. That is, one can imagine a situation in Møller scattering ($e^-e^-\to e^-e^-$), for example, in which the exchange of a real, physical photon is cut off (the relevant Fock state is the $e^-e^-\gamma$ intermediate state) but the exchange of an instantaneous photon is not (there is no intermediate state in this graph). We can avoid this problem with gauge invariance by considering the instantaneous photon in the instananeous photon-exchange graph to have quantum numbers as if it were a real photon. One then cuts it off in a manner similar to the Fock-state cutoff for a real intermediate state. That is, one requires

$$\sum_i \frac{k_{\perp i}^2+m_i^2}{x_i} \leq \Lambda^2 , \tag{3.6}$$

where the sum is over the individual particles in the Fock state *plus* the instantaneous photon. A similar procedure is taken for the instantaneous fermion interaction so the correct Feynman S-matrix amplitudes are restored in this sector also. As a concrete example, consider the graphs involved in Møller scattering shown in Fig. 3. Assume k_1^+ is larger than k_3^+. In the first graph, the photon's momenta are fixed by momentum conservation, and the three-particle intermediate state is cut off by

$$\frac{k_{3\perp}^2+m_e^2}{x_3}+\frac{k_{2\perp}^2+m_e^2}{x_2}+\frac{q_\perp^2}{x_q} \leq \Lambda^2 . \tag{3.7}$$

In the second graph, one *assigns* momenta to the instantaneous photon, $q^+=k_1^+-k_3^+$, $\mathbf{q}_\perp=\mathbf{k}_{1\perp}-\mathbf{k}_{3\perp}$, and then requires

$$\frac{k_{3\perp}^2+m_e^2}{x_3}+\frac{k_{2\perp}^2+m_e^2}{x_2}+\frac{q_\perp^2}{x_q} \leq \Lambda^2 . \tag{3.8}$$

With this requirement, whenever the instantaneous photon-exchange graph occurs, a corresponding graph with the exchange of a real, intermediate photon occurs

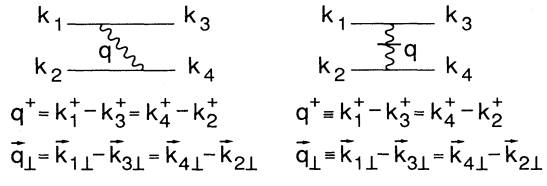

FIG. 3. Light-cone perturbation theory graphs contributing to Møller scattering. k_1^+ is assumed to be larger than k_3^+.

because both graphs are now cutoff in exactly the same way. As shown in Appendix A, the sum of the graphs is simply the gauge-invariant Feynman rules answer, $1/q_F^2$. Thus, we see that this method maintains gauge invariance of the ultraviolet cutoff for two-particle scattering at the tree level. It is not clear if this conclusion can be carried over to loop diagrams [44].

Similarly, to reproduce the form of the Feynman amplitude, we also adopt the same procedure for instantaneous fermions: the instantaneous graph is only retained if the corresponding propagating fermion graph contributes in the truncated theory.

We have now completed the ultraviolet regularization of light-cone theory. All Fock states are cut off by requiring the invariant mass squared to be less than Λ^2:

$$\sum_i \frac{k_{\perp i}^2+m_i^2}{x_i} \leq \Lambda^2 . \tag{3.9}$$

With this restriction, the Fock space is rendered finite, the ultraviolet regulation is invariant under the light-cone Lorentz transformations, and for two-particle scattering, the Born amplitudes are gauge invariant and are consistent with the Feynman form up to the cutoff. We also note that this regulation procedure is continuum regulator: the cutoff condition is not changed by discretization.

In principle, the global or kinetic cutoff can be used as the sole ultraviolet regulator needed to define the renormalized theory. However, these regulators have the disadvantage that, at finite Λ, the renormalization constants will depend on the kinematics of the "spectator" particles in the Fock state, rather than just the particles participating in the UV-divergent self-energy and vertex subgraphs. However, one still has the option of introducing further UV regulation such as massive Pauli-Villars particles [44] or massive supersymmetric partners to produce counterterms which render these subgraphs finite. We illustrate this method in Appendix C. Alternatively, one can also directly regulate the matrix elements of the interaction Hamiltonian such that [45] $\langle n|H_{\rm LC}|m\rangle=0$ if

$$\left|\sum_{i\in m}\frac{k_{\perp i}^2+m_i^2}{x_i}-\sum_{i\in n}\frac{k_{\perp i}^2+m_i^2}{x_i}\right| \geq \Lambda^2 .$$

When using any of these "local" cutoffs, the mass counterterms can be defined independently of the bound-state wave function, as in the standard treatment of the Lamb shift in QED [46]. The counterterms at a specific renormalization scale are chosen so that one obtains the physical values of the electron mass and photon mass when solving the light-cone equation of motion in the respective quantum number sector [47].

IV. COVARIANT INFRARED REGULATOR

There are a number of potential sources of infrared singularities and divergences in light-cone quantized QED. These are (1) singularities in H_0 and the three-point interactions from fermions with $x=0$ ($k^+=0$), (2) singularities at $x=0$ and divergences near $x=0$ from photons in H_0 and the three-point interactions, (3) the singularity from the exchange of an instantaneous fer-

mion at $x=0$, and (4) the singularity at $x=0$ and the divergence near $x=0$ from the exchange of an instantaneous photon.

The singularity described in item (1) can be removed by requiring antiperiodic boundary conditions for the fermions in the x^- direction. Similarly, the singularity in item (3) is removed if the fermions obey antiperiodic boundary conditions and the photons periodic boundary conditions because the momentum exchange will never be zero. Recall that the instantaneous fermion interaction is proportional to $1/q^+$, where $q^+=k^+_{\text{outgoing photon}}-k^+_{\text{incoming fermion}}$.

The singularity arising from photons with $x=0$ [point (2)] is eliminated by the cutoff described in the previous section if $\mathbf{q}_\perp\neq\mathbf{0}_\perp$ because the invariant mass squared of such a photon would be greater than any finite Λ^2. That is,

$$\frac{q_\perp^2}{x}>\Lambda^2 \tag{4.1}$$

for $q^+=0$. The case of $\mathbf{q}_\perp=\mathbf{0}_\perp$ is dealt with below. The singularity from instantaneous photons at $x=0$ [point (4)] and $\mathbf{q}_\perp\neq\mathbf{0}_\perp$ is eliminated because instantaneous photons are treated for purposes of the cutoff as if they were real photons. As a result, they are also eliminated because

$$\frac{q_\perp^2}{x}>\Lambda^2\ , \tag{4.2}$$

where q^+ and $\mathbf{q}_\perp$ are assigned to the instantaneous photon according to momentum conservation as explained in Sec. III. Again, the situation for $\mathbf{q}_\perp=\mathbf{0}_\perp$ is described below.

If periodic boundary conditions had been chosen for the fermions instead of antiperiodic conditions, the singularities at $x=0$ for real and instantaneous fermions would be eliminated by the same reasoning as for real and instaneous photons.

The divergence as x approaches 0 for real and instantaneous photons is removed by invoking an infrared cutoff:

$$\frac{q_\perp^2}{x}\geq\epsilon\ . \tag{4.3}$$

All states with real photons not satisfying this condition and all instantaneous photon interactions not meeting this criterion are removed. Once again, q^+ and $\mathbf{q}_\perp$ for a real Fock-state photon are taken to be their actual values; q^+ and $\mathbf{q}_\perp$ for an instantaneous photon are assigned according to momentum conservation as if it were a real photon.

Note that if ϵ is chosen to be any value smaller than $(\pi/L_\perp)^2$ but greater than 0, then the only effect of the infrared cutoff is to remove photons with $\mathbf{q}_\perp=\mathbf{0}_\perp$. Since the effect of the cutoff is identical for all ϵ less than $(\pi/L_\perp)^2$, one may as well take the limit $\epsilon\to 0$ right away. Since the point $\mathbf{q}_\perp=\mathbf{0}_\perp$ has now been removed, the problem of the $x=0$ singularity for real and instantaneous photons with zero $\mathbf{q}_\perp$ described above has been taken care of. Another way of removing the point $x=0$ when $\mathbf{q}_\perp=\mathbf{0}_\perp$ is to imagine that the photon has a small mass λ. Then $x=0$ would be eliminated for all $\mathbf{q}_\perp$ by the ultraviolet cutoff, Eq. (3.1).

The infrared cutoff is only necessary for numerical reasons when one uses a discrete measure. In the continuum, the spectrum and wave function of positronium has no infrared divergence. The numerical problem is illustrated in Fig. 4, which shows the divergent behavior of the lowest-energy level in a variational calculation as K is increased if one does not use an infrared cutoff. Details of this calculation are described in Ref. [38]. An explanation for this behavior is that the integral that must be reproduced to obtain the ground-state energy level

$$\langle\psi_0|H_{\text{LC}}|\psi_0\rangle=M_0^2 \tag{4.4}$$

has an integrand that diverges like

$$\frac{1}{x(q_\perp^2+m_e^2)-q_\perp^2} \tag{4.5}$$

for small $x,\mathbf{q}_\perp$. Of course, the integral itself is still finite. In the continuum, the points near $x=0$, $\mathbf{q}_\perp=\mathbf{0}_\perp$ are a set of measure zero and give a finite contribution to the integral. Unfortunately, in the discrete case, any one Fock state has a finite measure since there are only a finite number of Fock states. Each $(e^+e^-\gamma)$ Fock state contributes one point to the sum, Eq. (4.4). As a result, the Fock states with photon x near zero and $\mathbf{q}_\perp=\mathbf{0}_\perp$ give a contribution proportional to $1/x\sim K$. Thus, photons with $\mathbf{q}_\perp=\mathbf{0}_\perp$ must be removed by an infrared cutoff such as Eq. (4.3) to keep the sum Eq. (4.4) finite as $K\to\infty$.

Another way to eliminate this difficulty is to add and subtract an appropriate term in the Hamiltonian which removes the discretized infrared divergence and replaces this term at small $q_\perp$ and x by the appropriate continuum value. This method will be discussed in detail in Ref. [6].

In summary, an infrared regulator is included by requiring that all photons, real and instantaneous, have invariant mass squared greater that ϵ:

$$\frac{q_\perp^2}{x}\geq\epsilon\ . \tag{4.6}$$

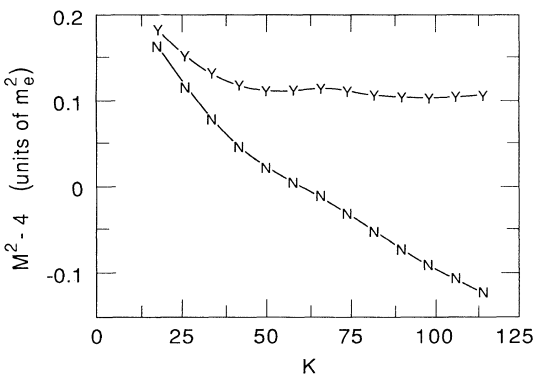

FIG. 4. Comparison of ground state energy with (Y) and without (N) infrared cutoff.

This Lorentz-invariant (tree level), gauge-invariant regulator ensures that all infrared divergences are well defined and cancel in a charge-zero system such as positronium. The numerical demonstration for this last state is given in Ref. [6]. Since the only effect of the cutoff is to remove photons with $\mathbf{q}_\perp=\mathbf{0}_\perp$ for any $0<\epsilon<(\pi/L_\pi)^2$, the limit $\epsilon\to 0$ can be taken immediately. Also note that this infrared regulator is a continuum condition: the cutoff requirement is unaffected by discretization.

V. TRUNCATED FOCK SPACE

The basic problem for solving QED_{3+1} using DLCQ has now been given: The light-cone Hamiltonian and bound-state equation are given in Sec. II, ultraviolet regularization is described in Sec. III, and infrared regularization in Sec. IV. There are several problems which still need to be confronted.

One must choose a consistent scheme for truncating the Fock space in order to have a system with finite number of degrees of freedom. In the case of one space and one-time theories, the parameter K automatically provides this truncation. In the case of physical theories in three space and one time, the covariant global and kinetic cutoffs defined in Sec. III provide a physically motivated cutoff. Unlike the Tamm-Dancoff [1] truncation, there is no *a priori* fixed limit on the number of particles in this scheme. Such a Fock-space truncation also provides a continuum regularization for renormalization. Unlike lattice gauge theories, this cutoff can be performed independent of the discretization. Ideally one should use ultraviolet regulators such as dimensional regularization in $d^2k_\perp$ or a generalized Pauli-Villars scheme [25]. The Fock-space truncation of the regulated theory then has only a mild effect at higher Λ^2.

However, a more fundamental problem is that, as of yet, no nonperturbative prescription is available for renormalization to all orders in closed form. This problem needs to be answered before the full QED_{3+1} light-cone Hamiltonian can be systematically diagonalized. An example of the construction of a nonperturbative counterterm is presented in the next section.

A simple nontrivial approximation to QED_{3+1} which retains its all-orders nonperturbative features is the Tamm-Dancoff [1] truncation to just two classes of Fock states on the light cone. To be specific, for the charge=zero sector, the Fock space will be limited to just (e^+,e^-) and (e^+,e^-,γ). For the charge-one sector, the only Fock states will be (e^-) and (e^-,γ). The number of interactions effectively allowed in this truncated Fock space is very much reduced from the full set shown in Fig. 1. All graphs involving pair creation are effectively removed because the truncated Fock space does not allow for extra fermion pairs (diagrams 3, 6, 9, 11, 12, 17, 18, and 19). Diagrams 14, 16, 20, and 21 are effectively removed because they involve two photons in flight. Finally, diagram 10 is eliminated when it occurs in the presence of a spectator photon because such a situation also has two photons in flight. Taking all these removals into account, the only diagrams that need be considered are 1, 2, 4, 5, 10, 13, and 15.

Limiting the Fock space may bring gauge invariance into question. However, we have carefully made sure that every time an intermediate state with real photons is removed, the corresponding intermediate state with instantaneous photons is also removed. This restores gauge invariance because photons are thus removed from the theory in gauge-invariant sets. For example, the interaction $e^+e^-\to\gamma\to e^+e^-$ is removed from consideration because the intermediate state with one real photon has been eliminated. To restore gauge invariance, we have been careful to drop diagram 9 which involves the same process, but through an instantaneous photon.

It should be emphasized that although the Fock space is limited, the analysis remains nonperturbative because the allowed Fock states can be iterated as many times as one wishes. In particular, keeping only $(e^+e^-,e^+e^-\gamma)$ is similar to the ladder approximation in Bethe-Salpeter methods, which is an all-orders calculation. Since this approximation has been solved in Bethe-Salpeter formalism for the spectrum of positronium, diagonalizing the light-cone QED Hamiltonian in this truncated Fock space must also reproduce the positronium spectrum. It is shown in Ref. [6] that the Bohr spectrum and the hyperfine splitting of positronium (actually, the muonium spectrum, since the annihilation channel has been removed) at large $\alpha\sim 0.3$ are correctly reproduced to leading order in α.

VI. RENORMALIZATION: SELF-INDUCED INERTIAS AND MASS COUNTERTERMS

Two issues are of concern regarding renormalization. First is the question of the self-induced inertias that appear in the theory if one does not normal order the light-cone Hamiltonian. The second is whether the light-cone perturbation theory results for the one-loop radiative corrections agree with the usual Feynman S matrix answers. Let us investigate the first question.

If one begins with a Hamiltonian that is not normal ordered and proceeds to normal order, one finds extra terms arising from interchanging operators in the instantaneous photon and instantaneous fermion interactions. These terms have been referred to in Refs. [3] and [32] as "self-induced inertias" and have been the source of much discussion concerning their role in light-cone physics. In QED_{3+1}, these extra terms take the form

$$\frac{2\alpha}{L_\perp^2}\sum_{\lambda,\underline{p}} a^\dagger_{\lambda,\underline{p}} a_{\lambda,\underline{p}} J_p,$$
$$J_p=\frac{1}{2p}\sum_{\underline{m}}(\{p-m\,|p-m\}-\{p+m|p+m\}) \tag{6.1}$$

for the photon and

$$\frac{2\alpha}{L_\perp^2}\left[\sum_{s,\underline{n}} b^\dagger_{s,\underline{n}} b_{s,\underline{n}}(I_n+K_n)+d^\dagger_{s,\underline{n}} d_{s,\underline{n}}(I_n+M_n)\right],$$
$$I_n=\tfrac{1}{2}\sum_{\underline{m}}([n-m|n-m]-[n+m|n+m]),$$
$$K_n=\tfrac{1}{2}\sum_{\mathbf{q}}\frac{1}{q}\{n-q|n-q\}, \tag{6.2}$$
$$M_n=\tfrac{1}{2}\sum_{\mathbf{q}}\frac{1}{q}\{n+q|n+q\},$$

for the fermion. Remember that, for fermion antiperiodic boundary conditions and photon periodic conditions,

$$p,q=2,4,6,\ldots, \quad m,n=1,3,5,\ldots . \tag{6.3}$$

The question then arises: Should the self-induced inertias remain in the theory or should they be removed? Simply starting with a normal-ordered Hamiltonian eliminates these inertias. A satisfactory answer for the truncated Fock space we are considering is that they are *not* needed; i.e., they are replaced by the mass counterterms below. In the case of the fermion, this counterterm happens to have the same continuum limit as the original self-induced inertia in the limit $\Lambda\to\infty$. The correct procedures for all Λ that properly renormalizes the fermion mass in the truncated Fock space requires mass counterterms equal to the one-loop light-cone perturbation theory mass counterterms. It should be noted that this result, which will be detailed below, only holds in the truncated space $(e^+e^-,e^+e^-\gamma)$ or $(e^-,e^-\gamma)$.

In our truncated Fock space, the full set of proper one-loop radiative corrections is shown in Fig. 5 (improper graphs do not need to be renormalized). Again, there is no vacuum polarization because the Fock space does not allow an extra fermion pair to be created. Mass counterterms are needed to cancel these self-mass diagrams. The discretized counterterms are

$$\delta H_{\rm LC}^{(1)} = -\underset{\substack{\rightarrow\\ n,\mathbf{n}_\perp}}{\sim\!\sim\!\sim}$$

$$=K\frac{2\alpha}{L_\perp^2}\sum_{q,\mathbf{q}_\perp}\frac{\dfrac{1}{2n(n-q)}\left[n^2\left[\mathbf{q}_\perp-\dfrac{q}{n}\mathbf{n}_\perp\right]^2+q^2\beta_f\right]+\dfrac{n^2}{q^2}\left[\mathbf{q}_\perp-\dfrac{q}{n}\mathbf{n}_\perp\right]^2}{n^2\left[\mathbf{q}_\perp-\dfrac{q}{n}\mathbf{n}_\perp\right]^2+q^2\beta_f+n(n-q)\beta_\gamma} \tag{6.4}$$

$$\delta H_{\rm LC}^{(2)} = -\sum_{N=2}^{\infty}\ \underset{\substack{\rightarrow\\ n,\mathbf{n}_\perp}}{\sim\!\overset{1}{\sim}\!\overset{2}{\sim}\!\cdots\!\sim\!\overset{N}{\sim}}$$

$$=-K\frac{\beta_f\pi^2}{nL_\perp^2}\frac{\left[\dfrac{\alpha}{\pi^2}\displaystyle\sum_{q,\mathbf{q}_\perp}\frac{q}{n^2\left[\mathbf{q}_\perp-\frac{q}{n}\mathbf{n}_\perp\right]^2+q^2\beta_f+n(n-q)\beta_\gamma}\right]^2}{1+\dfrac{\alpha}{\pi}\displaystyle\sum_{q,\mathbf{q}_\perp}\frac{n-q}{n^2\left[\mathbf{q}_\perp-\frac{q}{n}\mathbf{n}_\perp\right]^2+q^2\beta_f+n(n-q)\beta_\gamma}}, \tag{6.5}$$

where

$$\beta_f=\left[\frac{m_eL_\perp}{\pi}\right]^2,\quad \beta_\gamma=\left[\frac{\lambda L_\perp}{\pi}\right]^2,\quad \alpha=\frac{e^2}{4\pi},$$

$$\begin{aligned} &n=1,3,5,\ldots \text{ (antiperiodic BC)},\\ &q=2,4,6,\ldots,\\ &n^i,q^i=0,\pm1,\pm2,\ldots . \end{aligned} \tag{6.6}$$

$(n,\mathbf{n}_\perp)$ are the quantum numbers for the incoming fermion and λ is a fake photon mass that is ultimately set equal to zero. The sum is over $2\le q\le n-1$ and must satisfy both the ultraviolet and infrared cutoffs:

$$\frac{q_\perp^2+\beta_\gamma}{q}+\frac{(\mathbf{n}_\perp-\mathbf{q}_\perp)^2+\beta_f}{n-q}\le\frac{1}{K}\left[\frac{\Lambda L_\perp}{\pi}\right]^2-\sum_{\rm spec}\frac{m_\perp^2+\beta}{m}, \tag{6.7}$$

$$\frac{q_\perp^2+\beta_\gamma}{q}\ge\frac{1}{K}\left[\frac{L_\perp}{\pi}\right]^2\epsilon .$$

The sum in the first equation is over the quantum numbers $(m,\mathbf{m}_\perp)$ of all the spectator particles (i.e., particles that go from the initial to final state without an interaction). The derivation of these results is given in Appendix B. Note that, when one uses the Fock-space truncation as a regulator, one must take into account the unavoidable dependence on the spectator kinematics for any finite cutoff.

Inclusion of these mass counterterms and diagonalizing the space $(e^-,e^-\gamma)$ reproduces the real electron mass to be one to 12 significant figures on an IBM 3090 running 64-bit (double precision) real variables and thus verifies that this is indeed the correct fermion mass renormalization prescription. The numerical results are discussed further in Sec. VII. If self-induced inertias are retained, the mass counterterm is modified to include self-induced inertias. This just cancels the original inertias and diagonalizing again reproduces the real electron mass $=1.000\ldots m_e$.

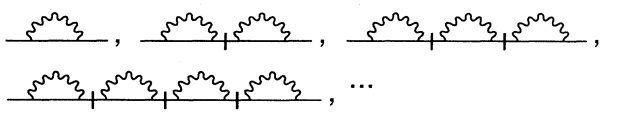

FIG. 5. One-loop LCPT radiative corrections to fermion line.

Let us now return to the second question posed at the beginning of this section. The equivalence of the mass counterterms derived from the usual covariant Feynman theory and light-cone perturbation theory is discussed in Appendix C. It is shown there that the infinite-momentum-frame time-ordered perturbation theory (TOPT_∞) and Feynman rules results for the one-loop fermion self-energy in Feynman gauge are identical if one is careful to do the x integral first and interchange limit and integral only when allowed in the TOPT_∞ calculation. If one takes the limit first, one obtains the non-Z graph as the complete answer, which agrees with the usual light-cone perturbation theory (LCPT) answer for the one-loop fermion self-energy, but disagrees with the Feynman answer. The discrepancy is found in a nonzero contribution from the Z graph in TOPT_∞ near $x=0$. The LCPT and Feynman rules answers for the one-loop fermion self-energy agree if an extra piece equal to the TOPT_∞ Z graph is added to the diagonal part of the light-cone Hamiltonian. This has to be done since the Z-graph contribution to the fermion self-energy is not obtained from the off-diagonal matrix elements of the light-cone Hamiltonian. However, since this piece is a self-energy, it is canceled when one includes the corresponding mass counterterm.

In practice, the extra piece from the Z graph can thus be ignored. It should be emphasized that, in the above deliberations, λ is only included as an infrared regulator and is at the end taken to be zero. The conclusions do not carry over to theories with a true massive photon.

This completes the discussion of electron mass renormalization. Because of the absence of pair creation, there is no renormalization arising from vacuum polarization in the truncated Fock-space consideration. This leaves just electron wave-function renormalization, which is equivalent to simply stating that the real electron's wave function is normalized. The probability of finding the bare Fock electron inside the real electron is given by the expansion coefficient ψ_{e^-} for the single-electron Fock state shown in Eq. (2.17). This coefficient is just the wave-function renormalization constant $\sqrt{Z_2}$.

To summarize, there is no photon wave-function renormalization (charge renormalization) in the truncated Fock space $(e^+e^-,e^+e^-\gamma)$ or (e^-,e^-,γ). Electron wave-function renormalization is automatic because the real electron's wave function is normalized. If one is careful about the behavior near the end points, $x=0,1$, the one-loop self-mass corrections in TOPT_∞ and LCPT agree with the answer from S-matrix analysis. Mass renormalization is then done by inserting mass counterterms into H_{LC} that exactly cancel the one-loop self-mass contributions. If one decides to keep the "self-induced inertias," these are also canceled by mass counterterms. Since the self-mass end-point corrections and self-induced inertias are just canceled anyway, what one effectively does is start with a normal-ordered Hamiltonian (i.e., without self-induced inertias) and inserts the mass counterterms given in Eqs. (6.4) and (6.5). Once again, this prescription is valid only in the truncated Fock space of one additional photon. If higher Fock states are included, a more general method is necessary which may, in fact, include the self-induced inertias in a crucial way.

Since only elementary particles require renormalization, no further renormalization needs to be done. That is, there is no positronium mass or wave-function renormalization. The full light-cone Hamiltonian given by Eqs. (2.2)–(2.7) plus mass counterterms given by Eqs. (6.4) and (6.5) is now ready to be diagonalized.

VII. DIAGONALIZATION: CHARGE-ONE SPACE

The prescription for diagonalizing the QED light-cone bound-state equation (2.20) is then the following. H_{LC} is equal to $H_0+H_1+H_2+H_{\mathrm{self}}$, where H_0, H_1, and H_2 were given in Eqs. (2.2)–(2.7) and H_{self} is the mass counterterms given in Eqs. (6.4) and (6.5). The Fock space is generated by keeping all Fock states that satisfy

$$\sum_i \frac{k_{\perp i}^2+m_i^2}{x_i} \leq \Lambda^2 \tag{7.1}$$

and have photons that satisfy

$$\frac{q_\perp^2}{x} \geq \epsilon \ . \tag{7.2}$$

These two cutoff conditions are also applied to the instantaneous fermion and photon interactions with the instantaneous particles treated as if they were real particles. Diagonalizing gives the full mass spectrum of states and their corresponding wave functions as a Fock-state expansion:

$$|\psi\rangle = \sum_n \psi_n(x,\mathbf{k}_\perp)|n\rangle \ . \tag{7.3}$$

In principle, the true continuum theory is recovered by taking the limits $K,L_\perp,\Lambda\to\infty$ and $\epsilon\to 0$. Recall from Sec. IV that the results are identical for any choice of ϵ less than $(\pi/L_\perp)^2$; therefore, one is allowed to take the limit $\epsilon\to 0$ immediately. In this paper, the Fock space is limited for various reasons discussed in Sec. V to just (e^-,e^-,γ) for charge one and (e^+e^-,e^+e^-,γ) for charge zero.

Diagonalizing the light-cone Hamiltonian in the charge-one space of (e^-,e^-,γ) for any value of α, K, $L_\perp$, Λ, and ϵ reproduces

$$M^2=1.000\ldots m_e^2 \tag{7.4}$$

for the ground state. Remember that, as pointed out in Sec. V, in this truncated Fock-space consideration, diagram 14 must be dropped from the full set of light-cone diagrams in Fig. 1. The accuracy of this result is only limited by machine precision. On an IBM 3090 running 64-bit real variables, this is 12 places behind the decimal point. This result demonstrates numerically that fermion mass renormalization is being done correctly in the truncated space $(e^-,e^-\gamma)$ because the physical mass of the fermion (i.e., the ground-state mass M) is reproduced.

One also obtains the fermion's structure function by summing the ground-state wave function over all modes with a fixed x:

$$f(x)=\sum_{n,\mathbf{k}_\perp,\lambda,\text{ fixed } x}|\psi_n(x,\mathbf{k}_\perp,\lambda)|^2 . \tag{7.5}$$

A typical structure function for $\alpha=0.3$ is shown in Fig. 6. As expected, the structure function is peaked at $x=1$ and has a characteristic long radiative tail.

VIII. SUMMARY

Discretized light-cone quantization has been presented as a fully relativistic discrete representation of quantum field theories and has been demonstrated to work, in principle, for quantum electrodynamics in three space and one time dimensions. Covariant (tree-level), gauge-invariant ultraviolet and infrared regularization were presented in Secs. III and IV and a complete renormalization scheme in the truncated Fock space of $(e^-,e^-\gamma)$ or $(e^+e^-,e^+e^-\gamma)$ was outlined in Sec. VI. The numerical check of the renormalization method is the demonstration that the electron's bare mass is equal to its physical mass using diagonalization. This is presented in Sec. VII.

Most of the positronium spectrum is contained in this truncated Fock space: The Bohr levels, $L\cdot S$ coupling, the hyperfine interaction, and the part of the Lamb shift from the fermion self-energy diagram are all included (the results obtained in this truncated Fock space will actually be for muonium because the annihilation potential is not present).

A possible method of extending this procedure to include the Fock state with two photons, $(e^+e^-\gamma\gamma)$, is to include mass counterterms for the fermion self-mass diagrams with two photons in flight. A subset of these are shown in Fig. 7. Including this Fock state with two photons should reproduce the full Lamb shift excluding the Uehling term for vacuum polarization. The Uehling term can be included by further extending the Fock state to include $(e^+e^-e^+e^-)$. This extension can be implemented by introducing photon-mass counterterms for the graphs in Fig. 8. As explained in Appendices D and E of Ref. [38], photon-mass counterterms are necessary because we are using a nonsubtractive ultraviolet regularization scheme. A test of whether this is done correctly is to check that the ground state has $M^2=0$. This would

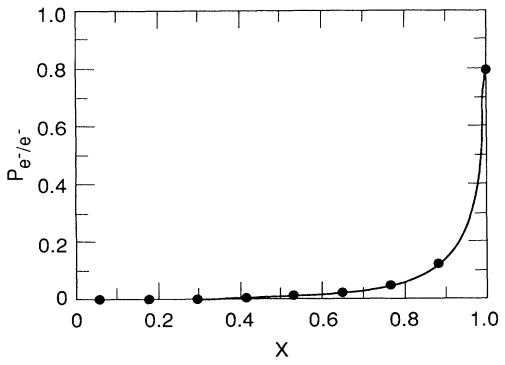

FIG. 6. Fermion structure function from diagonalization. $\alpha=0.3$, $K=17$, $L_\perp=101/m_e$, $\Lambda=2.3m_e$.

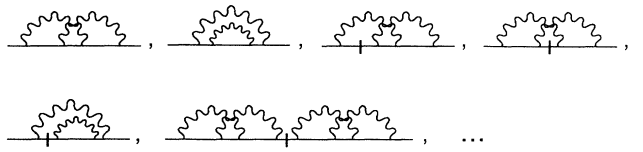

FIG. 7. Some fermion mass counterterms needed to include the $(e^+e^-\gamma\gamma)$ Fock state.

verify that the bare photon mass remains equal to the physical photon mass. Including this extra Fock state also puts back the annihilation potential needed to calculate true positronium levels.

The method of DLCQ has a number of important positive attributes.

(1) The technique is straightforward, nonperturbative, fully relativistic, and can be applied to quantum field theories in general, the most obvious candidate being quantum chromodynamics. Even the truncated Fock-space analysis is nonperturbative since the Fock states that are allowed are iterated an infinite number of times.

(2) Because of the positivity of P^+, there are no interactions in the theory that create massive particles out of the vacuum. As a result, in theories without zero modes, the vacuum structure is simple: the perturbative vacuum, which is the Fock-state vacuum, is also the true vacuum, the eigenstate of $H_{\rm LC}$ with $M^2=0$. An illuminating analysis of the influence of zero modes in QED_{1+1} has been given by Werner, Heinzl, and Krusche [48,49]. They show that, although it is correct to impose the gauge condition $A^+=0$ on the particle sector of the Fock space, one must allow for $A^+\neq 0$ if $k^+=0$. Allowing for this degree of freedom, one obtains a series of topological θ vacua on the light cone which reproduce the known features of the massless Schwinger model including a nonzero chiral condensate. However, the effect of the infrared zero-mode quanta decouples from the physics of zero-charge bound states, so that the physical spectrum in one space, one time gauge theories is independent of the choice of vacuum. The freedom in having a nonzero value for A^+ at $k^+=0$ can also be understood by using the gauge $\partial^+A^+\sim k^+A^+=0$ [24].

(3) Diagonalization has the potential of giving the full spectrum of bound states and scattering states along with their respective wave functions. Unlike equal time theory [50], the structure functions and distribution amplitudes needed in calculations of high-energy scattering processes can be obtained directly from the light-cone wave functions.

(4) The fermions are treated in a natural way. There are no fermion determinants or fermion doubling.

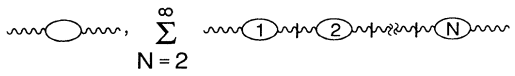

FIG. 8. Photon-mass counterterms needed to include the $(e^+e^-e^+e^-)$ Fock state.

(5) An $A^+=0$ gauge, there are only two physical photon polarizations.

After the validation of the DLCQ method to QED_{3+1}, the natural extension will be to QCD, particularly for heavy-quark systems. Unlike the situation for QED, it is anticipated that zero-mode quanta will be important for understanding the light-cone vacuum for QCD in physical space time. In particular, the non-Abelian four-point interaction term

$$H_{\rm int}^{\rm LC}=-\tfrac{1}{2}g^2\int d^3\underline{x}\ {\rm Tr}([A^\mu,A^\nu][A_\mu,A_\nu]) \tag{8.1}$$

plays a unique and an essential role, since $H_{\rm int}^{\rm LC}|0\rangle$ can be nonzero if one includes zero-mode gluons in the Fock space. Thus, the true light-cone vacuum $|\Omega\rangle$ is not necessarily identical to the perturbative vacuum $|0\rangle$. In fact, the zero-mode excitations of $H_I^{\rm LC}$ produce a color-singlet gluon condensate $\langle\Omega|G_{\mu\nu}G^{\mu\nu}|\Omega\rangle\neq 0$ of the type postulated in the QCD sum-rule analyses [51]. The effect of such condensates will be to introduce "soft" insertions into the quark and gluon propagators and their effective masses $m(p^2)$, and to modify the perturbative interactions at large distances. Thus, unlike the one space, one time theory, the zero-mode gluon excitations do affect the color-singlet bound states. The DLCQ method will have to be extended to include the possibility of zero-mode contributions in QCD_{3+1}. On the other hand, such zero-mode corrections to vacuum cannot appear in Abelian QED_{3+1} as long as a nonzero fermion mass appears in the free Hamiltonian.

The DLCQ method clearly as many advantages for solving nonperturbative problems in field theory. Many technical problems have been solved on how to regulate and renormalize gauge the Hamiltonian form of gauge theories quantized on the light cone. The true test of this procedure will be in the numerical applications. Results for the spectrum and bound-state wave functions for positronium at large α are given in Ref. [6]. Initial applications of DLCQ to QCD_{3+1} at low Fock class number have recently been made by Kaluza [52] and by Hollenberg *et al.* [53] in addition to our efforts.

ACKNOWLEDGMENTS

We wish to thank many colleagues at SLAC and MPI-Heidelberg for many helpful discussions and suggestions, especially Mathias Burkardt, Kent Hornbostel, Matjaz Kaluza, Michael Krautgärtner, Alex Langnau, and Frank Wölz. This work was supported by the Department of Energy, Contract No. DE-AC03-76SF00515.

APPENDIX A

In this appendix the tree-level Møller scattering amplitude ($e^-e^-\to e^-e^-$) derived using Feynman's S-matrix approach is shown to be identical to that derived from light-cone perturbation theory. The rules for LCPT are given in Appendix B in Ref. [14] and Appendix A in Ref. [25] and can be derived from the light-cone Hamiltonian $H_{\rm LC}$ given in Eqs. (2.2)–(2.7).

The diagrams that must be considered in LCPT are given in Fig. 9 with light-cone time x^+ flowing from left to right and momenta assigned as shown. Using P^+ and $\mathbf{P}_\perp$ momentum conservation, q and q' are

$$\begin{aligned} q^+&=l_i^+-l_f^+=k_f^+-k_i^+\ ,\\ \mathbf{q}_\perp&=\mathbf{l}_{\perp i}-\mathbf{l}_{\perp f}=\mathbf{k}_{\perp f}-\mathbf{k}_{\perp i}\ ,\\ q^-&=\frac{q_\perp^2+\lambda^2}{q^+}\ ,\\ q^{\mu'}&=-q^\mu\ . \end{aligned} \tag{A1}$$

Note that the photon's four-momentum q is on mass shell. Remember that P^- is not necessarily conserved, so

$$q^-\neq l_i^--l_f^-\neq k_f^--k_i^-\ . \tag{A2}$$

Using the LCPT rules found in Ref. [14] or [25] and performing the sum over photon polarizations, gives the following for the three LCPT graphs:

$$\begin{aligned} T_{fi}^{(1)}&=e^2\bar u(l_f)\gamma_\mu u(l_i)\bar u(k_f)\gamma_\nu u(k_i)\frac{\eta^\mu\eta^\nu}{(q^+)^2}\ ,\\ T_{fi}^{(2)}&=e^2\theta(q^+)\bar u(l_f)\gamma_\mu u(l_i)\bar u(k_f)\gamma_\nu u(k_i)\\ &\quad\times\left[-g^{\mu\nu}+\frac{\eta^\mu q^\nu+\eta^\nu q^\mu}{q^+}\right]\\ &\quad\times\frac{1}{q^+(l_i^--l_f^-)-q^+q^-+i\epsilon}\ ,\\ T_{fi}^{(3)}&=e^2\theta(-q^+)\bar u(l_f)\gamma_\mu u(l_i)\bar u(k_f)\gamma_\nu u(k_i)\\ &\quad\times\left[-g^{\mu\nu}+\frac{\eta^\mu q^\nu+\eta^\nu q^\mu}{q^+}\right]\\ &\quad\times\frac{1}{-q^+(k_i^--k_f^-)-q^+q^-+i\epsilon}\ , \end{aligned} \tag{A3}$$

where $\eta^\mu=(0,2,\mathbf{0}_\perp)$. Note that $T_{fi}^{(1)}$ diverges like $1/(q^+)^2$ for small q^+. The sum of these three amplitudes is

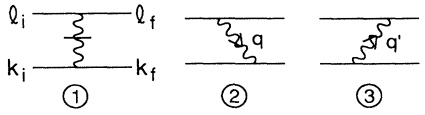

FIG. 9. Three graphs that occur in LCPT for tree-level Møller scattering.

$$T_{fi}=e^2 A_\mu B_\nu \left[\frac{\eta^\mu \eta^\nu}{(q^+)^2} + \left[-g^{\mu\nu} + \frac{\eta^\mu q^\nu + \eta^\nu q^\mu}{q^+} \right] \left[\frac{\theta(q^+)}{q^+(l_i^- - l_f^-) - q^+ q^- + i\epsilon} + \frac{\theta(-q^+)}{-q^+(k_i^- - k_f^-) - q^+ q^- + i\epsilon} \right] \right] , \tag{A4}$$

$$A_\mu = \bar{u}(l_f)\gamma_\mu u(l_i), \quad B_\nu = \bar{u}(k_f)\gamma_\nu u(k_i) ,$$

Writing out the components $\mu,\nu=+,-,1,2$ explicitly, one finds, after some algebra,

$$A_\mu B_\nu \theta(q^+) \left[\frac{\eta^\mu \eta^\nu}{(q^+)^2} + \frac{\eta^\mu q^\nu + \eta^\nu q^\mu}{q^+} \frac{1}{q^+(l_i^- - l_f^-) - q^+ q^- + i\epsilon} \right]$$

$$= A_\mu B_\nu \frac{\theta(q^+)}{q^+} \frac{1}{q^+(l_i^- - l_f^-) - q^+ q^- + i\epsilon} [\eta^\mu (l_i - l_f)^\nu + \eta^\nu (l_i - l_f)^\mu] . \tag{A5}$$

This expression can be summed with a similar expression for the $\theta(-q^+)$ term to give

$$\begin{aligned} T_{fi} = {} & e^2 \bar{u}(l_f)\gamma_\mu u(l_i)\bar{u}(k_f)\gamma_\nu u(k_i) \\ & \times \left[-g^{\mu\nu} \left[\frac{\theta(q^+)}{q^+(l_i^- - l_f^-) - q_\perp^2 - \lambda^2 + i\epsilon} + \frac{\theta(-q^+)}{q^+(k_f^- - k_i^-) - q_\perp^2 - \lambda^2 + i\epsilon} \right] \right. \\ & + \theta(q^+) \frac{\eta^\mu (l_i - l_f)^\nu + \eta^\nu (l_i - l_f)^\mu}{q^+} \frac{1}{q^+(l_i^- - l_f^-) - q_\perp^2 - \lambda^2 + i\epsilon} \\ & \left. + \theta(-q^+) \frac{\eta^\mu (k_f - k_i)^\nu + \eta^\nu (k_f - k_i)^\mu}{q^+} \frac{1}{q^+(k_f^- - k_i^-) - q_\perp^2 - \lambda^2 + i\epsilon} \right] . \end{aligned} \tag{A6}$$

This result is valid for on- or off-shell electrons and does not assume P^- momentum conservation. Note that this final expression for T_{fi} diverges only like $1/q^+$ for small q^+. The leading $1/(q^+)^2$ behavior from $T_{fi}^{(1)}$ is apparently canceled by a similar singularity from $T_{fi}^{(2)}$ and $T_{fi}^{(3)}$.

The Feynman answer can be obtained by first enforcing four-momentum conservation (i.e., $k_i^- + l_i^- = k_f^- + l_f^-$),

$$\begin{aligned} T_{fi} = {} & e^2 \bar{u}(l_f)\gamma_\mu u(l_i)\bar{u}(k_f)\gamma_\nu u(k_i) \\ & \times \frac{1}{q^+(l_i^- - l_f^-) - q_\perp^2 - \lambda^2 + i\epsilon} \\ & \times \left[-g^{\mu\nu} + \frac{\eta^\mu (l_i - l_f)^\nu + \eta^\nu (l_i - l_f)^\mu}{q^+} \right] , \end{aligned} \tag{A7}$$

and then requiring the electrons to be on shell [i.e., $\bar{u}(l_f)(\not{l}_i - \not{l}_f)u(l_i) = \bar{u}(k_f)(\not{l}_i - \not{l}_f)u(k_i) = \cdots = 0$]:

$$T_{fi} = -e^2 \bar{u}(l_f)\gamma_\mu u(l_i)\bar{u}(k_f)\gamma_\nu u(k_i) \frac{g^{\mu\nu}}{q_{\rm FR}^2 - \lambda^2 + i\epsilon} . \tag{A8}$$

$q_{\rm FR}^\mu$ is defined to be $l_i^\mu - l_f^\mu = k_f^\mu - k_i^\mu$. The last answer is recognized as the familiar answer for Møller scattering using Feynman rules. Note that the above analysis only holds for small λ. The conclusions should not be carried over to finite λ theories.

APPENDIX B

The calculation of various self-mass diagrams is given in this appendix. The first to be considered is the familiar one-loop fermion self-mass diagram shown in Fig. 10. The various momenta are

$$\begin{aligned} p &= \left[xP, \frac{x^2 p_\perp^2 + m_e^2}{xP}, x\mathbf{p}_\perp \right] , \\ k_1 &= \left[yP, \frac{(\mathbf{k}_\perp + y\mathbf{p}_\perp)^2 + \lambda^2}{yP}, \mathbf{k}_\perp + y\mathbf{p}_\perp \right] , \\ k_2 &= \left[(x-y)P, \frac{[-\mathbf{k}_\perp + (x-y)\mathbf{p}_\perp]^2 + m_e^2}{(x-y)P}, -\mathbf{k}_\perp + (x-y)\mathbf{p}_\perp \right] . \end{aligned} \tag{B1}$$

The LCPT amplitude for this process is

$$T_{fi}=\frac{g^2}{16\pi^3}\frac{1}{P}\int_0^x dy\int d^2\mathbf{k}_\perp\frac{1}{y(x-y)}\frac{N}{D+i\epsilon},\quad N=\bar{u}(p)\not{\epsilon}u(k_2)\bar{u}(k_2)\not{\epsilon}^*u(p)\ ,$$
$$D=\frac{x^2p_\perp^2+m_e^2}{xP}-\frac{(\mathbf{k}_\perp+y\mathbf{p}_\perp)^2+\lambda^2}{yP}-\frac{[-\mathbf{k}_\perp+(x-y)\mathbf{p}_\perp]^2+m_e^2}{(x-y)P}\ . \tag{B2}$$

The rules for LCPT QED are derived in Appendix B in Ref. [14] and Appendix A in Ref. [25]. The photon spin sum can be done by using the relation

$$\sum_\lambda \epsilon_\lambda^\mu\epsilon_\lambda^{\nu*}=-g^{\mu\nu}+\frac{\eta^\mu q^\nu+\eta^\nu q^\mu}{q^+}\ , \tag{B3}$$

which holds for the spinors given in Eq. (2.10) with $\eta^\nu=(0,2,0_\perp)$. Doing the numerator algebra and simplifying the denominator produces the desired answer

$$T_{fi}=-\delta_{ss'}\frac{g^2}{8\pi^3}x\int_0^x dy\int d^2k_\perp\frac{\frac{1}{x(x-y)}(x^2k_\perp^2+y^2m_e^2)+\frac{2}{y^2}[x^2k_\perp^2+x(x-y)\lambda^2]}{x^2k_\perp^2+y^2m_e^2+\lambda^2x(x-y)-i\epsilon}\ . \tag{B4}$$

$\delta_{ss'}$ is a δ function between the incoming and outgoing fermion spins. Note that, as expected from Lorentz invariance, this answer is independent of $\mathbf{p}_\perp$. If one changes variables to $z=y/x$, one also finds that the answer is independent of P and x. Since T_{fi} evidently does not depend on any of the quantum numbers of the incoming fermion, T_{fi} can be considered to be a pure mass renormalization.

The quantities actually discretized are $x,y,\mathbf{p}'_\perp=x\mathbf{p}_\perp$, and $\mathbf{k}'_\perp=\mathbf{k}_\perp+y\mathbf{p}_\perp$ or $-\mathbf{k}_\perp+(x-y)\mathbf{p}_\perp$. The choice between these last two is irrelevant. Rewriting T_{fi} in terms of these quantities gives

$$T_{fi}=-\delta_{ss'}\frac{g^2}{8\pi^3}x\int_0^x dy\int d^2\mathbf{k}_\perp\frac{\frac{1}{x(x-y)}\left[x^2\left[\mathbf{k}'_\perp-\frac{y}{x}\mathbf{p}'_\perp\right]^2+y^2m_e^2\right]+\frac{2}{y^2}\left[x^2\left[\mathbf{k}'_\perp-\frac{y}{x}\mathbf{p}'_\perp\right]^2+x(x-y)\lambda^2\right]}{x^2\left[\mathbf{k}'_\perp-\frac{y}{x}\mathbf{p}_\perp\right]^2+y^2m_e^2+\lambda^2x(x-y)-i\epsilon}\ . \tag{B5}$$

This answer is discretized by replacing

$$x=\frac{n}{K},\ y=\frac{q}{K},\ \mathbf{p}'_\perp=\frac{\pi\mathbf{n}_\perp}{L_\perp},\ \mathbf{k}'_\perp=\frac{\pi\mathbf{q}_\perp}{L_\perp},\ \int dy=\frac{2}{K}\sum_q,\ \int d^2\mathbf{k}_\perp=\left[\frac{\pi}{L_\perp}\right]^2\sum_{\mathbf{q}_\perp}\ , \tag{B6}$$

where $\pi n/L$ and $\pi\mathbf{n}_\perp/L_\perp$ are the P^+ and $\mathbf{P}_\perp$ of the incoming fermion, respectively, and $q=2,4,6,\ldots$. A factor of $1/x$ is also necessary because, in the continuum, factors of $1/\sqrt{x}$ from external wave functions are conventionally associated with the wave functions themselves; whereas, in the discretized case, the factors of $1/\sqrt{x}$ are absorbed into P^-. These steps give the result

$$T_{fi}=-\delta_{ss'}K\frac{2\alpha}{L_\perp^2}\sum_{q,\mathbf{q}_\perp}\frac{\frac{1}{2n(n-q)}\left[n^2\left[\mathbf{q}_\perp-\frac{q}{n}\mathbf{n}_\perp\right]^2+q^2\beta_f\right]+\frac{n^2}{q^2}\left[\mathbf{q}_\perp-\frac{q}{n}\mathbf{n}_\perp\right]^2}{n^2\left[\mathbf{q}_\perp-\frac{q}{n}\mathbf{n}_\perp\right]^2+q^2\beta_f+n(n-q)\beta_\gamma}\ , \tag{B7}$$

where $\beta_f=(mL_\perp/\pi)^2$ and $\beta_\lambda=(\lambda L_\perp/\pi)^2$. The photon mass, λ, has been set equal to zero in the numerator in this last expression.

Ultraviolet and infrared regulators are implemented by requiring that the intermediate state in Fig. 10 satisfies

$$\sum_i\frac{k_{\perp i}^2+m_i^2}{x_i}\le\Lambda^2,\quad\frac{(\mathbf{k}_\perp+y\mathbf{p}_\perp)^2+\lambda^2}{y}\ge\epsilon\ , \tag{B8}$$

which, in terms of the discrete variables given above, reads

$$\frac{q_\perp^2+\beta_\gamma}{q}+\frac{(\mathbf{n}_\perp-\mathbf{q}_\perp)^2+\beta_f}{n-q}\le\frac{1}{K}\left[\frac{\Lambda L_\perp}{\pi}\right]^2-\sum_{\text{spec}}\frac{m_\perp^2+\beta}{m}\ ,\quad\frac{q_\perp^2+\beta_\gamma}{q}\ge\frac{1}{K}\left[\frac{L_\perp}{\pi}\right]^2\epsilon\ . \tag{B9}$$

Here, β_i is equal to $(m_iL_\perp/\pi)^2$. The sum is over any spectator particles that might occur during the process. The

correct mass counterterm that should be inserted in $H_{\rm LC}$ to ensure that the fermion's bare mass is equal to its physical mass is the negative of Eq. (B7), where the sum is over $q^i=0,\pm1,\pm2,\ldots$ and $q=2,4,6,\ldots,n-1$ that satisfy Eq. (B9).

The next self-mass diagram to consider is shown in Fig. 11. The momenta are assigned to be

$$
\begin{aligned}
p&=\left[xP,\frac{x^2p_\perp^2+m_e^2}{xP},x\mathbf{p}_\perp\right],\\
k_1&=\left[yP,\frac{(\mathbf{k}_\perp+y\mathbf{p}_\perp)^2+\lambda^2}{yP},\mathbf{k}_\perp+y\mathbf{p}_\perp\right],\\
k_2&=\left[(x-y)P,\frac{[-\mathbf{k}_\perp+(x-y)\mathbf{p}_\perp]^2+m_e^2}{(x-y)P},-\mathbf{k}_\perp+(x-y)\mathbf{p}_\perp\right],\\
l_1&=\left[zP,\frac{(\mathbf{l}_\perp+z\mathbf{p}_\perp)^2+\lambda^2}{zP},\mathbf{l}_\perp+z\mathbf{p}_\perp\right],\\
l_2&=\left[(x-z)P,\frac{[-\mathbf{l}_\perp+(x-z)\mathbf{p}_\perp]^2+m_e^2}{(x-z)P},-\mathbf{l}_\perp+(x-z)\mathbf{p}_\perp\right]
\end{aligned}
\tag{B10}
$$

and the answer in LCPT is

$$
\begin{aligned}
T_{fi}&=\frac{1}{2xP}\left[\frac{g^2}{16\pi^3}\right]^2\int_0^x dy\,dz\int d^2\mathbf{k}_\perp d^2\mathbf{l}_\perp\frac{1}{y(x-y)z(x-z)}\frac{N}{D},\\
N&=\bar u(p)\not\epsilon(l_1)u(l_2)\bar u(l_2)\not\epsilon(l_1)^*\gamma^+\not\epsilon(k_1)u(k_2)\bar u(k_2)\not\epsilon(k_1)^*u(p),\\
D&=\left[\frac{x^2p_\perp^2+m_e^2}{x}-\frac{(\mathbf{k}_\perp+y\mathbf{p}_\perp)^2+\lambda^2}{y}-\frac{[-\mathbf{k}_\perp+(x-y)\mathbf{p}_\perp]^2+m_e^2}{x-y}+i\epsilon\right]\\
&\quad\times\left[\frac{x^2p_\perp^2+m_e^2}{x}-\frac{(\mathbf{l}_\perp+z\mathbf{p}_\perp)^2+\lambda^2}{y}-\frac{[-\mathbf{l}_\perp+(x-z)\mathbf{p}_\perp]^2+m_e^2}{x-z}+i\epsilon\right].
\end{aligned}
\tag{B11}
$$

The numerator algebra is done by using the photon spin sum relation Eq. (B3), applying symmetric integration to eliminate various terms proportional to k^i and l^i (upon simplification, the denominator turns out to only involve $k_\perp^2$ and $l_\perp^2$), and making use of the spinor properties shown in Appendix D. The answer for the numerator

$$
N=8Pm_e^2\frac{zy}{x}\delta_{ss'},
\tag{B12}
$$

turns out to only have a contribution from the spin-flip interaction of $H_{\rm LC}$. The complete answer is then

$$
T_{fi}=\delta_{ss'}\left[\frac{m_eg^2}{8\pi^3}\int_0^x dy\int d^2\mathbf{k}_\perp\frac{y}{x^2k_\perp^2+y^2m_e^2+\lambda^2x(x-y)-i\epsilon}\right]^2.
\tag{B13}
$$

Again, changing variables to $z=y/x$ demonstrates that this result is independent of x, P, and $\mathbf{p}_\perp$ and is therefore a pure mass renormalization.

Next, consider the case of N one-loop fermion self-mass pieces all connected by instantaneous fermions shown in Fig. 12. As above, momenta are assigned and the LCPT answer is written down for T_{fi}. The numerator and denominator are both factorizable, giving an answer of

$$
T_{fi}^{(N)}=\left[\frac{g^2}{8\pi^3x}\int_0^x dy\int d^2\mathbf{k}_\perp\frac{1}{y}\frac{1}{(m_e^2/x)-(k_\perp^2+\lambda^2)/y-(k_\perp^2+m_e^2)/(x-y)+i\epsilon}\right]^{N-2}T_{fi}^{(2)},
\tag{B14}
$$

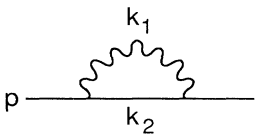

FIG. 10. One-loop fermion self-mass.

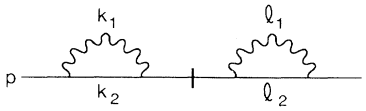

FIG. 11. One-loop fermion self-mass diagrams joined by instantaneous fermion.

where $T_{fi}^{(2)}$ is the answer for the diagram in Fig. 11. Using

$$\sum_{N=2}^{\infty} x^{N-2}=\frac{1}{1-x} \tag{B15}$$

and substituting in Eq. (B13) for $T_{fi}^{(2)}$ yields

$$T_{fi}=\delta_{ss'}\frac{m_e^2\left[\frac{g^2}{8\pi^3}\int_0^x dy\int d^2\mathbf{k}_\perp\frac{y}{x^2k_\perp^2+y^2m_e^2+\lambda^2x(x-y)-i\epsilon}\right]^2}{\frac{1+g^2}{8\pi^3}\int_0^x dy\int d^2\mathbf{k}_\perp\frac{x-y}{x^2k_\perp^2+y^2m_e^2+\lambda^2x(x-y)-i\epsilon}} \tag{B16}$$

as the amplitude for the process shown in Fig. 13. Similar to above, this result is discretized by rewriting in terms of x, y, $\mathbf{p}'_\perp=x\mathbf{p}_\perp$, and $\mathbf{k}'_\perp=\mathbf{k}_\perp+y\mathbf{p}_\perp$ and making the substitutions in Eqs. (B6) to give

$$T_{fi}=\delta_{ss'}K\frac{\beta_f\pi^2}{nL_\perp^2}\frac{\left[\frac{\alpha}{\pi^2}\sum_{q,\mathbf{q}_\perp}\frac{q}{n^2[\mathbf{q}_\perp-(q/n)\mathbf{n}_\perp]^2+q^2\beta_f+n(n-q)\beta_\gamma}\right]^2}{1+\frac{\alpha}{\pi^2}\sum_{q,\mathbf{q}_\perp}\frac{n-q}{n^2\left[\mathbf{q}_\perp-\frac{q}{n}\mathbf{n}_\perp\right]^2+q^2\beta_f+n(n-q)\beta_\gamma}} . \tag{B17}$$

This answer is subject to the same regularization conditions as above, Eq. (B9). The mass counterterm necessary in $H_{\rm LC}$ is the negative of Eq. (B17) subject to the conditions, Eq. (B9). A combination of the mass counterterms, Eqs. (B7) and (B17), provides the full mass renormalization needed in the truncated Fock space $(e^-,e^-\gamma)$ or $(e^+e^-,e^+e^-\gamma)$.

APPENDIX C

The equivalence of answers derived using Feynman's S-matrix analysis and using infinite-momentum-frame time-ordered perturbation theory is demonstrated in this appendix for the one-loop fermion self-energy diagram in Feynman gauge. Since it is believed that light-cone perturbation theory and TOPT$_\infty$ are mathematically equivalent, this demonstration makes the equivalence of LCPT and Feynman rules results for one-loop radiative corrections plausible. The analysis for the fermion self-energy is done in Feynman gauge for convenience, though the analysis should be similar in light-cone gauge in the limit $\lambda\to 0$.

First, the Feynman rules answer for the fermion self-energy graph shown in Fig. 14 is described briefly. We start with the familiar result

$$T_{fi}=-\frac{ig^2}{(2\pi)^4}\int d^4k\frac{\bar u(p)\gamma^\mu(\not p-\not k+m_e)\gamma_\mu u(p)}{[(p-k)^2-m_e^2+i\epsilon](k^2-\lambda^2+i\epsilon)} . \tag{C1}$$

A factor of $-i$ has been included to facilitate comparison with TOPT$_\infty$. Doing the numerator algebra, combining denominators, changing variables to $q^\mu=k^\mu-xp^\mu$, and eliminating terms proportional to q^μ by symmetric integration gives

$$T_{fi}=-\delta_{ss'}\frac{ig^2}{(2\pi)^4}\int d^4q\int_0^1 dx\frac{4m_e^2(1+x)}{(q^2-a^2+i\epsilon)^2} ,$$
$$a^2=m_e^2x^2+\lambda^2(1-x) . \tag{C2}$$

The δ function is between the spin of the incoming and outgoing fermion. Doing the q^0 integral by contour integration and then the q^3 integral by standard methods results in

$$T_{fi}=\delta_{ss'}\frac{g^2}{8\pi^3}\int_0^1 dx\int d^2\mathbf{q}_\perp\frac{2m_e^2(1+x)}{q_\perp^2+x^2m_e^2+\lambda^2(1-x)-i\epsilon} . \tag{C3}$$

This answer diverges like $\ln q_\perp^2$ for large $\mathbf{q}_\perp$; it is therefore necessary to introduce a regulator such as subtracting a Pauli-Villars contribution.

Now consider the same process in TOPT$_\infty$. The TOPT$_\infty$ rules for QED in Feynman gauge are given in Ref. [31]. Two graphs need to be considered, the usual time ordering and the Z graph. These are pictured in Fig. 15. Momenta are assigned to the various legs of the usual time-ordering contribution:

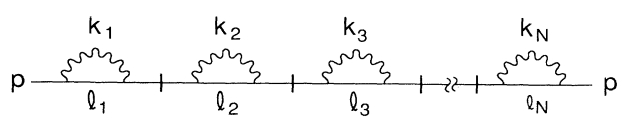

FIG. 12. N one-loop fermion self-mass pieces chained by $N-1$ instantaneous fermions.

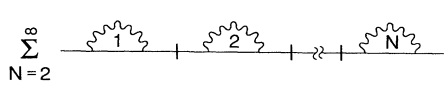

FIG. 13. Sum of N chained one-loop fermion self-mass diagrams.

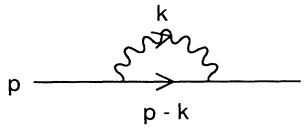

FIG. 14. One-loop fermion self-energy.

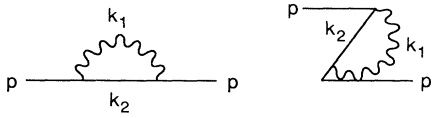

FIG. 15. One-loop fermion self-energy contributions in time-ordered perturbation theory. The right graph is typically referred to as the Z graph.

$$
\begin{aligned}
&p=(E,\mathbf{0}_\perp,P)\ ,\\
&k_1=(E_1,\mathbf{k}_\perp,xP)\ ,\\
&k_2=[E_2,-\mathbf{k}_\perp,(1-x)P]\ ,\\
&E=\sqrt{P^2+m_e^2}\ ,\\
&E_1=\sqrt{x^2P^2+\lambda_\perp^2}\ ,\\
&E_2=\sqrt{(1-x)^2P^2+m_\perp^2}\ ,\\
&\lambda_\perp^2=k_\perp^2+\lambda^2,\quad m_\perp^2=k_\perp^2+m_e^2.
\end{aligned}
\tag{C4}
$$

The time-ordered perturbation theory answer for this graph is

$$
T_{fi}=\frac{g^2}{4(2\pi)^3}P\int_{-\infty}^{\infty}dx\int d^2\mathbf{k}_\perp\frac{1}{E_1E_2}\frac{N}{D+i\epsilon}-(\lambda\to\Lambda)\ ,
\tag{C5}
$$

$$
N=\bar{u}(p)\not{\epsilon}u(k_2)\bar{u}(k_2)\not{\epsilon}^*u(p)\ ,
$$

$$
D=E-E_1-E_2\ .
$$

A Pauli-Villars contribution has been subtracted for ultraviolet regularization. The TOPT_∞ answer is gotten by letting P approach infinity, and the numerator is evaluated with the help of the relation

$$
\sum_\lambda \epsilon_\lambda^\mu\epsilon_\lambda^{\nu*}=-g^{\mu\nu}\ ,
\tag{C6}
$$

which holds in Feynman gauge. This gives the result

$$
T_{fi}=\lim_{P\to\infty}\delta_{ss'}\frac{g^2}{8\pi^3}\int_{-\infty}^{\infty}dx\int d^2\mathbf{k}_\perp[I(\lambda,P)-I(\Lambda,P)]\ ,
\tag{C7}
$$

$$
I(\lambda,P)=\frac{1}{\sqrt{x^2(\lambda_\perp/P)^2}\sqrt{(1-x)^2+(m_\perp/P)^2}}\frac{\sqrt{1+(m_e/P)^2}\sqrt{(1-x)^2+(m_\perp/P)^2}-(1-x)-2(m_e/P)^2}{\sqrt{1+(m_e/P)^2}-\sqrt{x^2+(\lambda_\perp/P)^2}-\sqrt{(1-x)^2+(m_\perp/P)^2}+i\epsilon}
$$

for the usual time ordering in $\mathrm{TOPT}_{\mathrm{inf}}$. Note that all the square roots are assumed to be *positive.*

The usual procedure is then to take the limit $P\to\infty$ inside the integral to simplify $I(\lambda,P)$. This is valid as long as one is not near the points $x=0,1$, which are singular for $P=\infty$. It is necessary to do a more detailed analysis near these two points. The integral is split into three regions: $x<0$, $0<x<1$, $x>1$.

(1) In the first region,

$$
E\to P[1+\tfrac{1}{2}(m/P)^2],\quad E_1\to -xP[1+\tfrac{1}{2}(\lambda_\perp/xP)^2]\ ,
$$

and

$$
E_2\to(1-x)P\{1+\tfrac{1}{2}[m_\perp/(1-x)P]^2\}
$$

as $P\to\infty$. $I(\lambda,P)$ approaches

$$
-\frac{1}{x(1-x)}\frac{\frac{1}{2}(1-x)(m_e^2/P^2)+\frac{1}{2}[m_\perp^2/(1-x)P^2]-2(m_e^2/P^2)}{2x}\underset{P\to\infty}{\to}0,
\tag{C8}
$$

which is nonsingular. Therefore, taking the limit before doing the x integration is allowed gives the result

$$
T_{fi}^{(1)}=0\ .
\tag{C9}
$$

(2) In this region,

$$
E\to P[1+\tfrac{1}{2}(m/P)^2],\quad E_1\to xP[1+\tfrac{1}{2}(\lambda_\perp/xP)^2]\ ,
$$

$$
E_2\to(1-x)P[1+\tfrac{1}{2}[m_\perp/(1-x)P]^2]\ ,
$$

and

$$I(\lambda,P)\to\frac{1}{x(1-x)}\frac{(1-x)m_e^2+[(k_\perp^2+m_e^2)/(1-x)]-4m_e^2}{m_e^2-[(k_\perp^2+\lambda^2)/x]-[(k_\perp^2+m_e^2)/(1-x)]+i\epsilon}$$
$$=\frac{1}{1-x}\frac{(1-x)^2m_e^2+k_\perp^2+m_e^2-4m_e^2(1-x)}{x(1-x)m_e^2-(1-x)(k_\perp^2+\lambda^2)-x(k_\perp^2+m_e^2)+i\epsilon} \tag{C10}$$

as $P\to\infty$. $I(\lambda,P)$ has a singularity near $x=1$. The integral for region (2) is split again into two parts:

$$T_{fi}^{(2)}=\lim_{\epsilon\to\infty}\lim_{P\to\infty}\delta_{ss'}\frac{g^2}{8\pi^3}\left[\int_0^{1-\epsilon}dx+\int_{1-\epsilon}^1 dx\right]\int d^2\mathbf{k}_\perp[I(\lambda,P)-I(\Lambda,P)]\ . \tag{C11}$$

(a) in the region $0<x<1-\epsilon$, we are away from the singularity so the limit $P\to\infty$ can be taken inside the integral to produce the answer

$$T_{fi}^{(2a)}=\lim_{\epsilon\to\infty}\delta_{ss'}\frac{g^2}{8\pi^3}\int_0^{1-\epsilon}dx\int d^2\mathbf{k}_\perp\frac{1}{x(1-x)}\frac{(1-x)m_e^2+[(k_\perp^2+m_e^2)/(1-x)]-4m_e^2}{m_e^2-[(k_\perp^2+\lambda^2)/x]-[(k_\perp^2+m_e^2)/(1-x)]+i\epsilon}-(\lambda\to\Lambda)\ . \tag{C12}$$

(b) The nonsingular part of $I(\lambda,P)$ is expanded in powers of $(1-x)$ to give the form

$$I(\lambda,P)=\frac{1}{\sqrt{(1-x)^2+(m_\perp/P)^2}}\sum_{n=0}^{\infty}A_n(\lambda,P)(1-x)^n \tag{C13}$$

for $I(\lambda,P)$. The contribution to T_{fi} is then

$$T_{fi}^{(2b)}=\lim_{\epsilon\to0}\lim_{P\to\infty}\delta_{ss'}\frac{g^2}{8\pi^3}\int_{1-\epsilon}^1 dx\int d^2\mathbf{k}_\perp\frac{1}{\sqrt{(1-x)^2+(m_\perp/P)^2}}\sum_{n=0}^{\infty}[A_n(\lambda,P)-A_n(\Lambda,P)](1-x)^n\ . \tag{C14}$$

Since λ and Λ appear in I only as λ/P and Λ/P, it must be that $A_n(\lambda,P)-A_n(\Lambda,P)$ approaches zero at least like $1/P$ as $P\to\infty$. One can expand A_n in powers of $1/P$ to see this. As $P\to\infty$, the *most* divergent x integral is

$$\int_{1-\epsilon}^{\epsilon}dx\frac{(1-x)^0}{\sqrt{(1-x)^2+(m_\perp/P)^2}}$$
$$=\ln\left[\frac{\epsilon+\sqrt{\epsilon^2+(m_\perp/P)^2}}{|m_\perp|/P}\right]\underset{P\to\infty}{\sim}\ln\frac{2\epsilon P}{|m_\perp|}\ . \tag{C15}$$

The final answer as $P\to\infty$ is then

$$T_{fi}^{(2b)}\to\frac{1}{P}\ln P\to0\ . \tag{C16}$$

(3) Finally, in the third region, $x>1$,

$$I(\lambda,P)\underset{P\to\infty}{\to}\frac{1}{x(1-x)}\ , \tag{C17}$$

which is singular near $x=1$. As above, the integral is split into two pieces: one for $1<x<1+\epsilon$ and one for $1+\epsilon<x<\infty$. In the first region, the nonsingular part of $I(\lambda,P)$ is expanded in powers of $(x-1)$, similar to Eq. (C13). Again, we find that $A_n(\lambda,P)-A_n(\Lambda,P)\to1/P$ as $P\to\infty$ and that the x integrals diverge at most like $\ln P$. Thus, this region gives a zero contribution to T_{fi}. The limit $P\to\infty$ can be taken inside the x integral for $1+\epsilon<x<\infty$ since we are away from the singularity to give

$$T_{fi}^{(3)}=\lim_{\epsilon\to0}\delta_{ss'}\frac{g^2}{8\pi^3}$$
$$\times\int_{1+\epsilon}^{\infty}dx\int d^2\mathbf{k}_\perp\left[\frac{1}{x(1-x)}-\frac{1}{x(1-x)}\right]$$
$$=0\ . \tag{C18}$$

The contributions from the three x regions are now summed to give the final answer for the usual time-ordering, one-loop fermion self-energy diagram:

$$T_{fi}=\delta_{ss'}\frac{g^2}{8\pi^3}\int_0^1 dx\int d^2\mathbf{k}_\perp\frac{1}{x(1-x)}\frac{(1-x)m_e^2+[(k_\perp^2+m_e^2)/(1-x)]-4m_e^2}{m_e^2-[(k_\perp^2+\lambda^2)/x]-[(k_\perp^2+m_e^2)/(1-x)]+i\epsilon}-(\lambda\to\Lambda)$$

$$=\delta_{ss'}\frac{g^2}{8\pi^3}\int_0^1 dx\int d^2\mathbf{k}_\perp\frac{1}{1-x}\frac{(2-2x-2x^2)m_e^2-k_\perp^2}{k_\perp^2+x^2m_e^2+(1-x)\lambda^2-i\epsilon}-(\lambda\to\Lambda). \tag{C19}$$

Note that this result diverges like Λ^2 for large Λ. A term

$$1=\frac{k_\perp^2+x^2m_e^2+(1-x)\lambda^2}{k_\perp^2+x^2m_e^2+(1-x)\lambda^2} \tag{C20}$$

can be added to the first term in the integrand and an analogous term with λ replaced by Λ subtracted from the second term to give

$$T_{fi}=\delta_{ss'}\frac{g^2}{8\pi^3}\int_0^1 dx\int d^2\mathbf{k}_\perp\frac{2m_e^2+\lambda^2}{k_\perp^2+x^2m_e^2+(1-x)\lambda^2-i\epsilon} -(\lambda\to\Lambda)\ . \tag{C21}$$

Now turn to the Z-graph contribution. A procedure similar to the above for the usual time ordering is applied. The momenta are assigned to be

$$\begin{aligned} p&=(E,\mathbf{0}_\perp,P)\ ,\\ k_1&=(E_1,\mathbf{k}_\perp,-xP)\ ,\\ k_2&=[E_2-\mathbf{k}_\perp,-(1-x)P]\ ,\\ E&=\sqrt{P^2+m_e^2}\ ,\\ E_1&=\sqrt{x^2P^2+\lambda_\perp^2}\ ,\\ E_2&=\sqrt{(1-x)^2P^2+m_\perp^2}\ ,\\ \lambda_\perp^2&=k_\perp^2+\lambda^2\ ,\\ m_\perp^2&=k_\perp^2+m_e^2\ . \end{aligned} \tag{C22}$$

The TOPT$_\infty$ result for the Z graph including Pauli-Villars regularization is

$$T_{fi}=\lim_{P\to\infty}\frac{g^2}{4(2\pi)^3}P\int_{-\infty}^{\infty}dx\int d^2\mathbf{k}_\perp\frac{1}{E_1E_2}\frac{N}{D+i\epsilon}-(\lambda\to\Lambda)\ ,$$

$$N=-\bar u(p)\not\epsilon^*v(k_2)\bar v(k_2)\not\epsilon u(p)\ , \tag{C23}$$

$$D=-E-E_1-E_2\ .$$

Doing the numerator algebra gives

$$T_{fi}=\lim_{P\to\infty}\delta_{ss'}\frac{g^2}{8\pi^3}\int_{-\infty}^{\infty}dx\int d^2\mathbf{k}_\perp[I(\lambda,P)-I(\Lambda,P)]\ , \tag{C24}$$

$$I(\lambda,P)=\frac{1}{\sqrt{x^2+(\lambda_\perp/P)^2}}\frac{1}{\sqrt{(1-x)^2+(m_\perp/P)^2}}\frac{\sqrt{1+(m_e/P)^2}\sqrt{(1-x)^2+(m_\perp/P)^2}+(1-x)+2(m_e/P)^2}{\sqrt{1+(m_e/P)^2}+\sqrt{x^2+(\lambda_\perp/P)^2}+\sqrt{(1-x)^2+(m_\perp/P)^2}-i\epsilon}\ .$$

Again, we find potential singularities in $I(\lambda,P)$ near $x=0,1$. The integral is again split into three regions: $x>1$, $0<x<1$, $x<0$.

(1) For $x>1$, $E\to P[1+\frac{1}{2}(m/P)^2]$, $E_1\to xP[1+\frac{1}{2}(\lambda_\perp/xP)^2]$, and $E_2\to(x-1)P\{1+\frac{1}{2}[m_\perp/(1-x)P]^2\}$ as $P\to\infty$ and

$$I(\lambda,P)\underset{P\to\infty}{\sim}\frac{1}{x(x-1)}\frac{\frac{1}{2}(x-1)(m_e^2/P^2)+\frac{1}{2}[m_\perp^2/(x-1)P^2]-2(m_e^2/P^2)}{2x}\to 0\ , \tag{C25}$$

which is nonsingular. The limit $P\to\infty$ can be taken inside to give

$$T_{fi}^{(1)}=0\ . \tag{C26}$$

(2) In the second region,

$$I(\lambda,P)\underset{P\to\infty}{\to}\frac{1}{x}\ , \tag{C27}$$

which is singular near $x=0$. The integral is split into two pieces:

$$T_{fi}^{(2)}=\lim_{\epsilon\to 0}\lim_{P\to\infty}\delta_{ss'}\frac{g^2}{8\pi^3}\left[\int_0^\epsilon dx+\int_\epsilon^1 dx\right]\int d^2\mathbf{k}_\perp[I(\lambda,P)-I(\Lambda,P)]\ . \tag{C28}$$

(a) The nonsingular part of $I(\lambda,P)$ is expanded in powers of x for the region $0<x<\epsilon$ to give

$$I(\lambda,P)=\frac{1}{\sqrt{x^2+(\lambda_\perp/P)^2}}\sum_{n=0}^{\infty}A_n(\lambda,P)x^n\ . \tag{C29}$$

Focus specifically on the contribution of the term A_0 to T_{fi},

$$T_{fi}^{(2a_0)}=\lim_{P\to\infty}\delta_{ss'}\frac{g^2}{8\pi^3}\int d^2\mathbf{k}_\perp\left[A_0(\lambda,P)\int_0^\epsilon\frac{dx}{\sqrt{x^2+(\lambda_\perp/P)^2}}-(\lambda\to\Lambda)\right]$$
$$=\lim_{P\to\infty}\delta_{ss'}\frac{g^2}{8\pi^3}\int d^2\mathbf{k}_\perp\left[A_0(\lambda,P)\ln\left[\frac{\epsilon+\sqrt{\epsilon^2+(\lambda_\perp/P)^2}}{|\lambda_\perp|/P}\right]-(\lambda\to\Lambda)\right]\ . \tag{C30}$$

As $P\to\infty$, $A_0(\lambda,P)$ and $A_0(\Lambda,P)$ both approach one and the log approaches $\ln(2\epsilon P/|\lambda_\perp|)$. Using these relations, we find

$$T_{fi}^{(2a_0)}=\delta_{ss'}\frac{g^2}{8\pi^3}\int d^2\mathbf{k}_\perp\ln\frac{|\Lambda_\perp|}{|\lambda_\perp|}$$
$$=\delta_{ss'}\frac{g^2}{16\pi^3}\int d^2\mathbf{k}_\perp\ln\frac{k_\perp^2+\Lambda^2}{k_\perp^2+\lambda^2}\ . \tag{C31}$$

Analysis of the other terms A_n, $n=1,2,3,\ldots$, reveals that their contribution to T_{fi} all approach zero as $P\to\infty$. So, the complete answer for the region $0<x<\epsilon$ is

$$T_{fi}^{(2a)}=\delta_{ss'}\frac{g^2}{16\pi^3}\int d^2\mathbf{k}_\perp\ln\frac{k_\perp^2+\Lambda^2}{k_\perp^2+\lambda^2}\ . \tag{C32}$$

(b) For $\epsilon<x<1$ the integrand is nonsingular, so the limit can be taken inside the integral to give

$$T_{fi}^{(2b)}=\delta_{ss'}\frac{g^2}{8\pi^3}\int_\epsilon^1 dx\int d^2\mathbf{k}_\perp\left[\frac{1}{x}-\frac{1}{x}\right]=0\ . \tag{C33}$$

(3) For $x<0$, the results are similar to $0<x<1$. There is a singularity in $I(\lambda,P)$ near $x=0$. Expanding I in powers of $-x$ for $-\epsilon<x<0$ reveals a contribution identical to Eq. (C32) from the term A_0. All other contributions vanish as $P\to\infty$. Summing contributions from $x>1$, $0<x<1$, and $x<0$ gives the total result

$$T_{fi}=\delta_{ss'}\frac{g^2}{8\pi^3}\int d^2\mathbf{k}_\perp\ln\frac{k_\perp^2+\Lambda^2}{k_\perp^2+\lambda^2} \tag{C34}$$

for the Z-graph contribution to the one-loop fermion self-energy diagram. This answer can be rewritten as

$$T_{fi}=\delta_{ss'}\frac{g^2}{8\pi^3}\int_0^1 dx\int d^2\mathbf{k}_\perp\frac{-\lambda^2+2m_e^2x}{k_\perp^2+x^2m_e^2+(1-x)\lambda^2-i\epsilon}$$
$$-(\lambda\to\Lambda). \tag{C35}$$

Note that this answer disagrees with the Z-graph answer using a naive application of the tree graph rule for including backward moving particles given in Refs. [31] and [13]. Of course, this rule continues to remain valid for tree graphs.

Summing this result with that for the usual time-ordering Equation (C21) yields an answer identical to the Feynman rules answer, Eq. (C3), demonstrating the equivalence of using TOPT_∞ and Feynman rules for the one-loop fermion self-energy. The final answer in TOPT_∞ is just the Feynman rules answer.

Summarizing, the usual time-ordering graph gives an answer in TOPT_∞ that diverges like Λ^2 and is equal to the usual LCPT answer for the fermion self-energy. There are no contributions to this graph from the regions near $x=0$ or 1. The Z-graph contribution in TOPT_∞ only has a contribution near $x=0$ and sums with the usual time-ordering graph to give the familiar Feynman rules answer. This final answer diverges like $\ln\Lambda$ because the leading Λ^2 divergence cancels. In order to reconcile the LCPT and Feynman rules answers for the one-loop fermion self-energy, an extra piece equal to the TOPT_∞ Z graph must be added to the light-cone Hamiltonian and the LCPT rules [54].

One final note: It should be noted that the method of implementing a Pauli-Villars ultraviolet regulator in Feynman gauge used above is not appropriate in light-cone gauge unless a modification is made. The problem in light-cone gauge is that the transverse degrees of freedom are mass dependent, but the longitudinal degree (i.e., the instantaneous interaction) is not. Consequently, the Pauli-Villars counterterm has (up to a sign) exactly the same instantaneous piece as the true photon, and (at least at the tree level) a suppressed transverse piece for large Λ. Therefore, the counterterm cancels the instantaneous piece and leaves the transverse piece unmodified as $\Lambda\to\infty$. The full answer at tree level would be just the transverse interaction, which is incorrect and not gauge invariant.

This problem can be remedied by introducing a dynamical longitudinal photon with derivative coupling proportional to the photon mass squared. However, since the photon mass is usually here only as an infrared regulator and is ultimately sent to zero, no consequences of significance arise from the improper treatment of the photon mass term in this work. Implementing a Pauli-Villars regulator in light-cone gauge would, however, require the addition of heavy longitudinal photons [55].

APPENDIX D

A set of useful spinor properties is given in this appendix. See also [13].

$\bar{u}(k,s)\cdots u(k,s')$	$\uparrow\to\uparrow$ $\downarrow\to\downarrow$	$(s'\to s)$	$\uparrow\to\downarrow$ $\downarrow\to\uparrow$
$\bar{u}u$	$2m_e$		0
$\bar{u}\gamma^\mu u$	$2k^\mu$		0
$\bar{u}\gamma^+\gamma^- u$	$4m_e$		$4(\pm k^1+ik^2)$
$\bar{u}\gamma^-\gamma^+ u$	$4m_e$		$4(\mp k^1-ik^2)$
$\bar{u}\gamma^+\gamma^i u$	0		$2k^+(\pm\delta^{i1}+i\delta^{i2})$
$\bar{u}\gamma^i\gamma^+ u$	0		$2k^+(\mp\delta^{i1}-i\delta^{i2})$
$\bar{u}\gamma^-\gamma^+\gamma^- u$	$8\left[\frac{k_\perp^2+m_e^2}{k^+}\right]$		0
$\bar{u}\gamma^-\gamma^+\gamma^i u$	$4(k^i\mp i\epsilon^{ij}k^j)$		$4m_e(\pm\delta^{i1}+i\delta^{i2})$
$\bar{u}\gamma^i\gamma^+\gamma^- u$	$4(k^i\pm i\epsilon^{ij}k^j)$		$4m_e(\mp\delta^{i1}-i\delta^{i2})$
$\bar{u}\gamma^i\gamma^+\gamma^j u$	$2k^+(\delta^{ij}\pm i\epsilon^{ij})$		0

$\bar{v}(k,s)v(k,s')=-2m_e\delta_{ss'}$

$\bar{v}(k,s)\gamma^\mu v(k,s')=2k^\mu\delta_{ss'}$

$\bar{v}(k,s)u(k,s')=\bar{u}(k,s)v(k,s')=0$

$\bar{u}(k,s)(\gamma^\mu\gamma^\nu\gamma^\sigma+\gamma^\sigma\gamma^\nu\gamma^\mu)u(k,s')=\bar{v}(k,s)(\gamma^\mu\gamma^\nu\gamma^\sigma+\gamma^\sigma\gamma^\nu\gamma^\mu)v(k,s')$
$=(4g^{\mu\nu}k^\sigma-4g^{\mu\sigma}k^\nu+4g^{\nu\sigma}k^\mu)\delta_{ss'}$

$\bar{v}(k,s)\gamma^\mu\gamma^\nu\gamma^\sigma v(k',s')=\bar{u}(k',s')\gamma^\sigma\gamma^\nu\gamma^\mu u(k,s)$

$i,j=1,2,\ \ \mu,\nu,\sigma=0,1,2,3$ or $+,-,1,2$

[1] I. Tamm, J. Phys. (Moscow) **9**, 449 (1945); S. M. Dancoff, Phys. Rev. **78**, 382 (1950).

[2] P. A. M. Dirac, Rev. Mod. Phys. **21**, 392 (1949).

[3] H. C. Pauli and S. J. Brodsky, Phys. Rev. D **32**, 1993 (1985); **32**, 2001 (1985).

[4] R. J. Perry, A. Harindranath, and K. G. Wilson, Phys. Rev. Lett. **65**, 2959 (1990); R. J. Perry and A. Harindranath, Phys. Rev. D **43**, 492 (1991).

[5] D. Mustaki, S. Pinsky, J. Shigemitsu, and K. Wilson, Phys. Rev. D **43**, 3411 (1991).

[6] M. Krautgärtner, H. C. Pauli, and F. Wölz, Heidelberg Report MPIH-V4-1991 (unpublished); H. C. Pauli (unpublished).

[7] J. R. Klauder, H. Leutwyler, and L. Streit, Nuovo Cimento **59**, 315 (1969).

[8] J. B. Kogut and D. E. Soper, Phys. Rev. D **1**, 2901 (1970).

[9] F. Rohrlich, Acta Phys. Austriaca, Suppl. **VIII**, 2777 (1971).

[10] H. Leutwyler, Nucl. Phys. **B76**, 413 (1974).

[11] A. Casher, Phys. Rev. D **14**, 452 (1976).

[12] S. J. Chang, R. G. Root, and T. M. Yan, Phys. Rev. D **7**, 1133 (1973); S. J. Chang and T. M. Yan, *ibid.* **7**, 1147 (1973).

[13] G. P. Lepage and S. J. Brodsky, Phys. Rev. D **22**, 2157 (1980); Phys. Lett. **87B**, 359 (1979); Phys. Rev. Lett. **43**, 545 (1979); **43**, 1625 (1979).

[14] S. J. Brodsky and C. R. Ji, in *Quarks and Leptons,* Proceedings of the Fourth South African Summer School, Stellenbosch, South Africa, 1985, edited by C. A. Engelbrecht, Lecture Notes in Physics Vol. 248 (Springer-Verlag, Berlin, 1986).

[15] G. P. Lepage, S. J. Brodsky, T. Huang, and P. B. Mackenzie, in *Particles and Fields—2,* Proceedings of the Banff Summer Institute, Banff, Canada, 1981, edited by A. Z. Capri and A. N. Kamal (Plenum, New York, 1983).

[16] G. McCartor, Z. Phys. C **41**, 271 (1988).

[17] E. V. Prokhvatilov and V. A. Franke, Yad. Fiz. **49**, 1109 (1989) [Sov. J. Nucl. Phys. **49**, 688 (1989)].

[18] V. A. Franke, Y. V. Novoshilov, and E. V. Prokhvatilov, Phys. Lett. Math. Phys. **5**, 239 (1981).

[19] A. M. Annenkova, E. V. Prokhvatilov, and V. A. Franke, Zielona Gora Pedag. University Report WSP-IF 89-01, 1990 (unpublished).

[20] V. A. Karmanov, Nucl. Phys. **B166**, 378 (1980).

[21] V. A. Karmanov, Nucl. Phys. **A362**, 331 (1981).

[22] V. N. Pervushin, Nucl. Phys. **B15**, 197 (1990).

[23] C. McCartor, Z. Phys. C **41**, 271 (1988).

[24] F. Lenz, in *Nonperturbative Quantum Field Theory,* Proceedings of the NATO Advanced Summer Institute, Cargese, France, 1989, edited by D. Vautherin, F. Lenz, and J. W. Negele, NATO Advanced Study Institute, Series B: Physics (Plenum, New York, 1990).

[25] G. P. Lepage, S. J. Brodsky, T. Huang, and P. B. Mackenzie, in *Particles and Fields—2,* (Ref. [15]).
[26] S. J. Brodsky and G. P. Lepage, in *Perturbative Quantum Chromodynamics,* edited by A. H. Mueller (World-Scientific, Singapore, 1989).
[27] S. Weinberg, Phys. Rev. **150**, 1313 (1966).
[28] S. D. Drell, D. Levy, and T. M. Yan, Phys. Rev. **187**, 2159 (1969); Phys. Rev. D **1**, 1035 (1970); **1**, 1617 (1970).
[29] L. Susskind, Phys. Rev. **165**, 1535 (1968); L. Susskind and G. Frye, *ibid.* **164**, 2003 (1967).
[30] J. D. Bjorken, J. B. Kogut, and D. E. Soper, Phys. Rev. D **3**, 1382 (1971); J. B. Kogut and D. E. Soper, *ibid.* **1**, 2901 (1970).
[31] S. J. Brodsky, R. Roskies, and R. Suaya, Phys. Rev. D **8**, 4574 (1973).
[32] T. Eller, H. C. Pauli, and S. J. Brodsky, Phys. Rev. D **35**, 1493 (1987).
[33] A. Harindranath and J. P. Vary, Phys. Rev. D **36**, 1141 (1987).
[34] K. Hornbostel, S. J. Brodsky, and H. C. Pauli, Phys. Rev. D **41**, 3814 (1990).
[35] M. Burkardt, Nucl. Phys. **A504**, 762 (1989).
[36] M. Burkardt and R. Busch, Stanford Linear Accelerator Center Report No. SLAC-PUB5426 (unpublished).
[37] J. R. Hiller, Phys. Rev. D **43**, 2418 (1991).
[38] A. C. Tang, Stanford Linear Accelerator Center Report No. SLAC-351, 1990 (unpublished).
[39] C. Hamer (private communication).
[40] The notation $\epsilon^{\perp}$ is introduced for notational clarity. It is equal to $\epsilon_{\perp}$.
[41] Here g is the charge of the fermion. If we identify the fermion as the positron in QED, then $g=|e|$.
[42] Since those boost operators that mix the minus and plus directions do not commute with the cutoff light-core Hamiltonian, not all symmetries are preserved by this truncation.
[43] See, e.g., P. Hoyer and S. J. Brodsky, Stanford Linear Accelerator Center Report No. SLAC PUB 5374, 1990 (unpublished).
[44] See also M. Burkardt and A. Langnau, Phys. Rev. D **44**, 1187 (1991).
[45] We thank G. P. Lepage for suggesting this method.
[46] D. R. Yennie, in *Brandeis Summer Lectures in Theoretical Physics* (Brandeis University, Waltham, MA, 1963), Vol. I.
[47] This method is also consistent with the "alternating denominator" method of Ref. [31] for the renormalization of perturbative QED in the Hamiltonian formalism. These methods and regularizations have recently been applied to two- and three-loop perturbative calculations. See A. Langnau (private communication).
[48] Th. Heinzl, St. Krusche, and E. Werner, Regensburg Report No. TPR 90-44 (unpublished). See also S. Glazek, Phys. Rev. D **38**, 3277 (1988).
[49] G. McCartor, Southern Methodist University report, 1991 (unpublished); K. Hornbostel, Cornell University Report No. CLNS-90-1038, 1990 (unpublished).
[50] A variational calculation of the low-lying spectrum at large α using an equal-time Fock expansion has been recently given by W. Dykshoorn, R. Koniuk, and R. Munoz-Tapia, Phys. Rev. A **41**, 60 (1991).
[51] For a review, see. V. L. Chernyak, A. R. Zhitnitskii, Phys. Rep. **112**, 173 (1984).
[52] M. Kaluza, Ph.D. thesis, University of Heidelberg, 1990.
[53] L. C. L. Hollenberg, K. Higashijima, R. C. Warner, and B. H. J. McKellar, National Laboratory for High Energy Physics Report No. KEK-TH-280, 1991 (unpublished).
[54] Although conceptually different, this procedure is effectively similar to the procedure of adding noncovariant counterterms to the light-cone Hamiltonian as suggested in Ref. [44].
[55] M. Burkardt (private communication).